TET is targeted for proteasomal degradation by the PHD-pVHL pathway to reduce DNA hydroxymethylation

Received for publication, May 25, 2020, and in revised form, September 19, 2020 Published, Papers in Press, September 22, 2020, DOI 10.1074/jbc.RA120.014538

Sijia Fan[1,2,‡], Jing Wang[1,2,3,4,5,‡], Guangqing Yu[1,2], Fangjing Rong[1,2], Dawei Zhang[1], Chenxi Xu[1], Juan Du[1], Zhi Li[1,2], Gang Ouyang[1,3,4,5], and Wuhan Xiao[1,2,3,4,5,*]

From the [1]State Key Laboratory of Freshwater Ecology and Biotechnology, Institute of Hydrobiology, Chinese Academy of Sciences, the [3]Key Laboratory of Aquatic Biodiversity and Conservation, Institute of Hydrobiology, Chinese Academy of Sciences, the [4]Key Laboratory of Aquaculture Disease Control, Ministry of Agriculture, Wuhan, China, the [2]University of Chinese Academy of Sciences, Beijing, China, and the [5]Innovation Academy of Seed Design, Chinese Academy of Sciences, Wuhan, China

Edited by George N. DeMartino

Hypoxia-inducible factors are heterodimeric transcription factors that play a crucial role in a cell's ability to adapt to low oxygen. The von Hippel-Lindau tumor suppressor (pVHL) acts as a master regulator of HIF activity, and its targeting of prolyl hydroxylated HIF-α for proteasomal degradation under normoxia is thought to be a major mechanism for pVHL tumor suppression and cellular response to oxygen. Whether pVHL regulates other targets through a similar mechanism is largely unknown. Here, we identify TET2/3 as novel targets of pVHL. pVHL induces proteasomal degradation of TET2/3, resulting in reduced global 5-hydroxymethylcytosine levels. Conserved proline residues within the LAP/LAP-like motifs of these two proteins are hydroxylated by the prolyl hydroxylase enzymes (PHD2/EGLN1 and PHD3/EGLN3), which is prerequisite for pVHL-mediated degradation. Using zebrafish as a model, we determined that global 5-hydroxymethylcytosine levels are enhanced in vhl-null, egln1a/b-double-null, and egln3-null embryos. Therefore, we reveal a novel function for the PHD-pVHL pathway in regulating TET protein stability and activity. These data extend our understanding of how TET proteins are regulated and provide new insight into the mechanisms of pVHL in tumor suppression.

Von Hippel-Lindau (*VHL*) is a classic tumor suppressor and is linked to human hereditary VHL diseases that are autosomal-dominant and neoplastic diseases, including clear cell renal cell carcinoma (ccRCC) (1). The best-characterized function of pVHL is as a substrate recognition subunit of the VCB E3 ligase complex, which targets the proline hydroxylated hypoxia-induced factors (HIF-1α and HIF-2α) for proteasomal degradation under normoxia (2). HIF-1α and HIF-2α, which are master regulators of the cellular response to O_2 (3, 4), modulate the expression of a wide array of genes involved in multiple biological processes in response to hypoxia. Therefore, targeting of HIF-α for proteasomal degradation is thought to be the major mechanism of tumor suppression of pVHL. However, targets other than HIF-α have been tentatively identified, including estrogen receptor α (5), Kruppel-like factor receptor 7 (6), ERK5 (7), E2F1(8), androgen receptor (9), MAVS (10), AKT (11), and ZHX2 (12). A role for additional targets of pVHL could contribute to multifarious nature of the symptoms exhibited in VHL disease.

Given that both DNA methylation and hypoxia are correlated with cancer initiation and progression (13, 14), the connection between hypoxia and DNA methylation has been a major focus of research, though the results have not always been consistent (15–19). Hypoxia has been shown to influence DNA methylation either by transcriptionally activating the ten-eleven translocation enzyme 1 (TET1) or by reducing TET activity (15, 19–21). The TET proteins (TET1, TET2, and TET3), which are key factors identified in DNA demethylation serve as methylcytosine dioxygenases that catalyze the successive oxidation of 5-methylcytosine to 5-hydroxymethylcytosine (5-hmC), 5-formylcytosine, and 5-carboxylcytosine (22–27). The TET proteins have important roles in various biological processes, including the regulation of gene expression, meiotic mitosis, embryogenesis, stem cell function, immunoregulation, and cancer (27). Recently, TET1 has also been revealed to affect hypoxia signaling through interaction with HIF-1α (28, 29). In addition, Fumarate and Succinate (30) have been shown to regulate the expression of hypoxia-inducible genes via TET enzymes. Therefore, TET proteins appear to affect hypoxia signaling reciprocally.

DNA demethylation is a critical step in gene expression, and TET proteins are key factors involved in this process. Thus, the regulation of TET proteins has been investigated at the post-translational level (31–37). IDAX and CXXC5 have been shown to interact with TET2 and regulate its stability through caspase-dependent degradation (31). Calpain 1 mediates TET1/2 turnover in mouse embryonic stem cells, and calpain 2 regulates TET3 levels during differentiation (34). Furthermore, p300 has been shown to mediate TET2 acetylation, resulting in the stabilization of TET2 by inhibition of ubiquitination (37). Consequently, by affecting TET protein stability, these factors can modulate DNA demethylation, which regulates gene expression (31, 34, 37). The identification of factors that modulate TET stability and the demonstration of the mechanisms underlying this modulation would greatly increase the understanding of the TET function. However, as a classic protein degradation pathway, ubiquitin-proteasome system–mediated proteolysis of TET proteins remains poorly understood (38, 39).

This article contains supporting information.

‡These authors contributed equally to this work.
*For correspondence: Wuhan Xiao, w-xiao@ihb.ac.cn.

Given the reciprocal effect of hypoxia signaling and TET proteins, we sought to determine whether pVHL, as a key component of the E3 ligase complex of hypoxia signaling complex, has an effect on TET protein stability and function in mediating DNA demethylation. In this study, we demonstrate that pVHL targets TET protein for proteasomal degradation. Moreover, the prolyl hydroxylation of TET proteins catalyzed by PHD2 and PHD3 is prerequisite for pVHL-mediated proteasomal degradation, revealing a mechanism of PHD-pVHL in regulating TET proteins that is similar to its mechanism in regulating HIF-α proteins.

Results

pVHL interacts with TET proteins

To test whether pVHL interacts with TET proteins, we performed co-immunoprecipitation assays. We cotransfected Myc-tagged pVHL (Myc-VHL) together with FLAG-tagged TET1/2/3 into HEK293T cells. FLAG-TET1/2/3 pulled down Myc-pVHL efficiently (Fig. S1*A* and Fig. 1, *A* and *B*). To confirm whether pVHL interacts with TET endogenously, we further performed co-immunoprecipitation assays using polyclonal anti-pVHL antibodies in H1299 cells, a nonsmall-cell lung carcinoma cell line that expresses endogenous pVHL, TET2/3. Compared with rabbit IgG, anti-pVHL antibody pulled down endogenous TET2/3 (Fig. 1*C*). Because of a lack of suitable anti-TET1 antibody, we could not confirm whether pVHL interacts with TET1 endogenously. Therefore, in subsequent assays, we focused our studies on pVHL modulating TET2/3.

pVHL induces proteasomal degradation of TET proteins

Given the well-characterized function of pVHL as a component of the VHL-elongin B/C E3 ligase complex (40), we sought to determine whether pVHL could mediate TET proteasomal degradation. Coexpression of FLAG-tagged pVHL together with HA-tagged TET2/3 in HEK293T cells caused a dramatic reduction of TET2 and TET3 protein levels in a dose-response manner, but the proteasomal inhibitor, MG132 (20 μM), blocked reduction of TET2/3 effectively (Fig. 1, *D* and *E*). Similarly, coexpression of pVHL together with HA-tagged TET1, FLAG-tagged TET2, or FLAG-tagged TET3 in HEK293T cells decreased the protein levels of TET1, TET2, and TET3 (Fig. S1, *B* and *C*). Consistently, overexpression of pVHL caused reduction of endogenous TET2/3 levels in H1299 cells, which were blocked by MG132 (20 μM) (Fig. 1*F*). In addition, overexpression of pVHL also caused reduction of endogenous TET2 levels in HEK293T cells (Fig. S1*D*). Conversely, knockdown of pVHL by VHL-shRNA in H1299 cells enhanced TET2/3 protein levels (Fig. 1*G*).

When the protein synthesis inhibitor cycloheximide (50 μg/ml) was added to the culture medium, the degradation rate of TET2/3 was faster when pVHL was coexpressed compared with the empty vector control, suggesting that the new protein synthesis was not required in this process (Fig. 1, *H* and *I*). Taken together, these data suggest that pVHL induces proteasomal degradation of TET proteins.

Of note, it has been reported that hypoxia enhances TET expression (resulted in increased 5-hmC) via HIF-dependent transactivation of TET1/2/3 (20, 21, 41). To determine whether degradation of endogenous TET2/3 by pVHL is caused by the effect of pVHL in suppression of HIF-dependent TET2/3 transactivation, we performed quantitative real time PCR assays (qPCR). As shown in Fig. S2*A*, overexpression of pVHL in H1299 cells could not diminish TET2/3 mRNA levels under normoxia, which agreed with the low protein levels of HIF-α in VHL-intact cell lines under normoxia (42). However, knockdown of pVHL by VHL-shRNA in H1299 cells increased TET2/3 mRNA levels in a dose-dependent manner under normoxia (Fig. S2*B*). Moreover, when the HIF-α–specific inhibitor 2-methoxyestradiol (2ME2) (50 μM) was added to the culture medium (43), the enhancement of TET2/3 mRNA levels by knockdown of pVHL disappeared (Fig. S2*C*). These data indicate that pVHL could indeed modulate TET expression via HIF-dependent transactivation. However, when the HIF-α function was blocked by 2ME2 (50 μM), knockdown of pVHL still clearly caused increases of endogenous TET2/3 protein levels (Fig. S2*D*), suggesting that pVHL could regulate TET stability at the protein level independent of HIF and regulate TET expression via HIF-dependent transactivation in H1299 cells as reported previously (20, 21, 41).

pVHL reduces TET enzymatic activity

TET is known to oxidize 5-methylcytosine to 5-hydroxymethylcytosine (5hmC) (23, 25), with subsequent formation of 5-formylcytosine and 5-carboxylcytosine (22, 44), and to trigger passive, DNA replication–dependent DNA demethylation (45, 46). To determine whether pVHL affects TET function, we examined global 5hmC levels by dot blot assays. Overexpression of pVHL in H1299 cells significantly decreased global 5hmC levels (Fig. 2, *A* and *B*; pCMV-VHL *versus* pCMV empty). By contrast, overexpression of TET2 increased global 5hmC levels (Fig. 2, *A* and *B*; HA-TET2 *versus* pCMV empty). Furthermore, the increase in global 5hmC levels was reversed by coexpression of pVHL together with TET2 (Fig. 2, *A* and *B*; HA-TET2 + pCMV-VHL *versus* HA-TET2). Similar results were observed for TET3 (Fig. 2, *C* and *D*). Conversely, transfection with VHL-shRNA increased the global 5hmC levels compared with transfection with GFP-shRNA (Fig. 2, *E* and *F*).

To determine whether pVHL affects global 5hmC levels via the HIF pathway, we blocked HIF-α function by adding 2ME2 (50 μM) to the culture medium (43) and examined global 5hmC levels through dot blot assays. When VHL was knocked down by transfection with VHL-shRNA, the global 5hmC levels in the cells were increased compared with the cells transfected with GFP-shRNA (Fig. S2, *E* and *F*). These results suggest that pVHL can affect TET activity independent of HIF.

Taken together, these data suggest that pVHL attenuates TET enzymatic activity, leading to reduction of global 5hmC levels, and that the effect of pVHL on TET activity appears to be independent of the HIF pathway.

PHD2/3 mediate TET2/3 protein degradation

pVHL targets prolyl hydroxylated HIF-1α or HIF-2α for proteasomal degradation under normoxia (40). In this process,

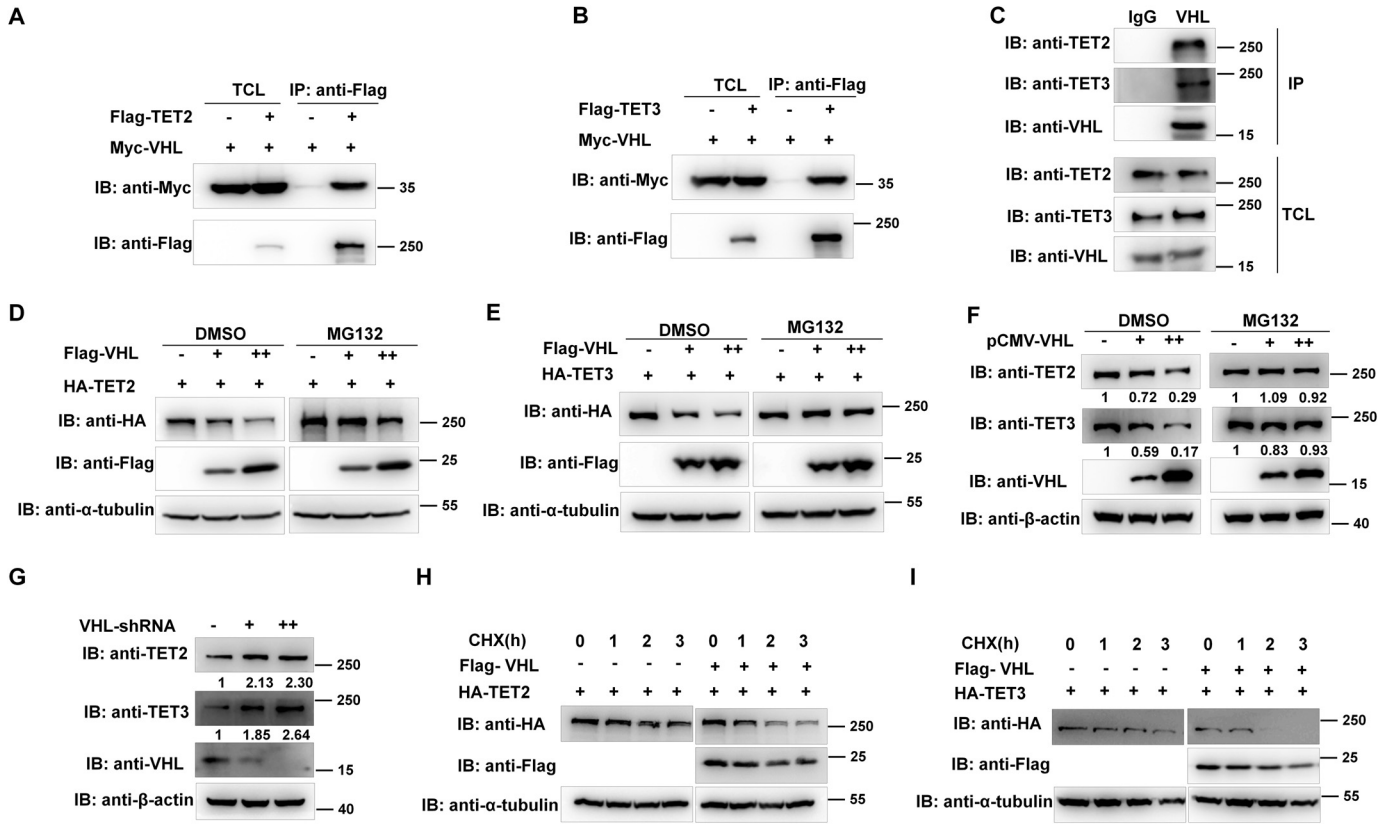

Figure 1. pVHL interacts with TET2/3 and induces TET2/3 degradation. *A* and *B*, pVHL interacts with TET2 or TET3. Co-immunoprecipitation of Myc–VHL with FLAG-TET2 or FLAG-TET3 in HEK293T cells transfected with the indicated plasmids. Anti-FLAG antibody was used for co-immunoprecipitation. *C*, endogenous pVHL interacts with endogenous TET2 or TET3 in H1299 cells. Anti-VHL antibody was used for co-immunoprecipitation, and rabbit IgG was used as control. *D* and *E*, pVHL induces degradation of TET2 or TET3, but the protein degradation is blocked by MG132. HEK293T cells were transfected with the indicated plasmids and harvested after transfection of 24 h; MG132 (20 μM) was added to the culture medium for 8 h before the cells were harvested; and the proteins were detected by Western blotting analysis. (−), the cells transfected with the empty vector control; (+), the cells transfected the indicted vector (1.0 μg); ($^{2+}$), the cells transfected with the indicated vector (2.0 μg). *F*, overexpression of pVHL induces degradation of endogenous TET2 or TET3 in H1299 cells, but the protein degradation is blocked by MG132. H1299 cells were transfected with pCMV-VHL and harvested after transfection of 24 h; MG132 (20 μM) was added to the culture medium for 8 h before cells were harvested, and the same amount of DMSO was used as a carrier control; the proteins were detected by Western blotting analysis. (−), the cells transfected with the empty vector control; (+), the cells transfected the indicted vector (1.0 μg); ($^{2+}$), the cells transfected with the indicated vector (2.0 μg). *G*, knockdown of VHL by pSuper-VHL-shRNA enhances endogenous TET2 and TET3 in H1299 cells. H1299 cells were transfected with pSuper-VHL-shRNA and harvested after transfection of 24h; the proteins were detected by Western blotting analysis. (−), the cells transfected with the empty vector control; (+), the cells transfected the indicted vector (2.0 μg); ($^{2+}$), the cells transfected with the indicated vector (4.0 μg). *H* and *I*, overexpression of pVHL reduces stabilization of TET2 or TET3 in the presence of cycloheximide (*CHX*; 50 μg/ml). HEK293T cells were transfected with the indicated plasmids for 24 h, then cycloheximide was added to the culture medium. At different time points, the cells were harvested for Western blotting analysis. *IB*, immunoblotting; *IP*, immunoprecipitation; *TCL*, total cell lysate.

HIF-α is hydroxylated by PHD (also called EGLN) prolyl hydroxylase enzymes (PHD1/EGLN2, PHD2/EGLN1, and PHD3/EGLN3) at conserved proline residues in the LAP motifs, which is required for pVHL-mediated proteasomal degradation (47, 48). Of note, TET proteins of human, mouse, and zebrafish contain similar LAP motifs or LAP-like motifs that are identical to those of HIF-1α and HIF-2α, in which the proline residues are evolutionarily conserved (Fig. S3). This similarity prompted us to assess whether the PHDs are also involved in pVHL-induced TET protein degradation. First, we cotransfected HA-tagged TET2/3 or versions of these proteins with proline mutated to alanine in the LAP/LAP-like motifs (TET2-Pro/Ala mutant, TET2-P1248A/P1255A; TET3-Pro/Ala mutant, TET3-P948A/P955A) together with PHD1 (HA-PHD1), PHD2 (FLAG-PHD2), or PHD3 (HA-PHD3). Cotransfection of PHD1 had no obvious effect on protein stability of TET2/3 and their mutants (TET2-Pro/Ala mutant and TET3-Pro/Ala mutant) (Fig. S4). However, cotransfection of PHD2/3 induced degradation of TET2/3 in a dose-dependent manner with no significant effect on their mutants (Fig. 3, *A–D*).

To gain insight into the mechanisms by which PHD2/3 induce TET2/3 degradation, we examined whether PHD2/3 interact with TET2/3 by co-immunoprecipitation assays. After cotransfection of Myc-tagged PHD proteins and FLAG-tagged TET proteins in HEK293T cells, anti-PHD2 antibody efficiently pulled down PHD2 and anti-FLAG antibody efficiently pulled down PHD3 (Fig. 3, *E, F, H,* and *I*). Moreover, anti-TET2/3 antibody could also pull down endogenous PHD2/3 in H1299 cells, suggesting physiological interaction between PHD2/3 and TET2/3 (Fig. 3, *G* and *J*).

To further determine whether PHD2/3-mediated TET2/3 degradation depends on PHD2/3 enzymatic activity, we used catalytically inactive PHD2 (PHD2-mut, PHD2-H290/351A) and PHD3 (PHD3-mut, PHD3-H135/196A) mutants (49–52). Compared with coexpression of WT PHD2 (PHD2-wt) or WT PHD3 (PHD3-wt), coexpression of PHD2 mutant (PHD2-mut)

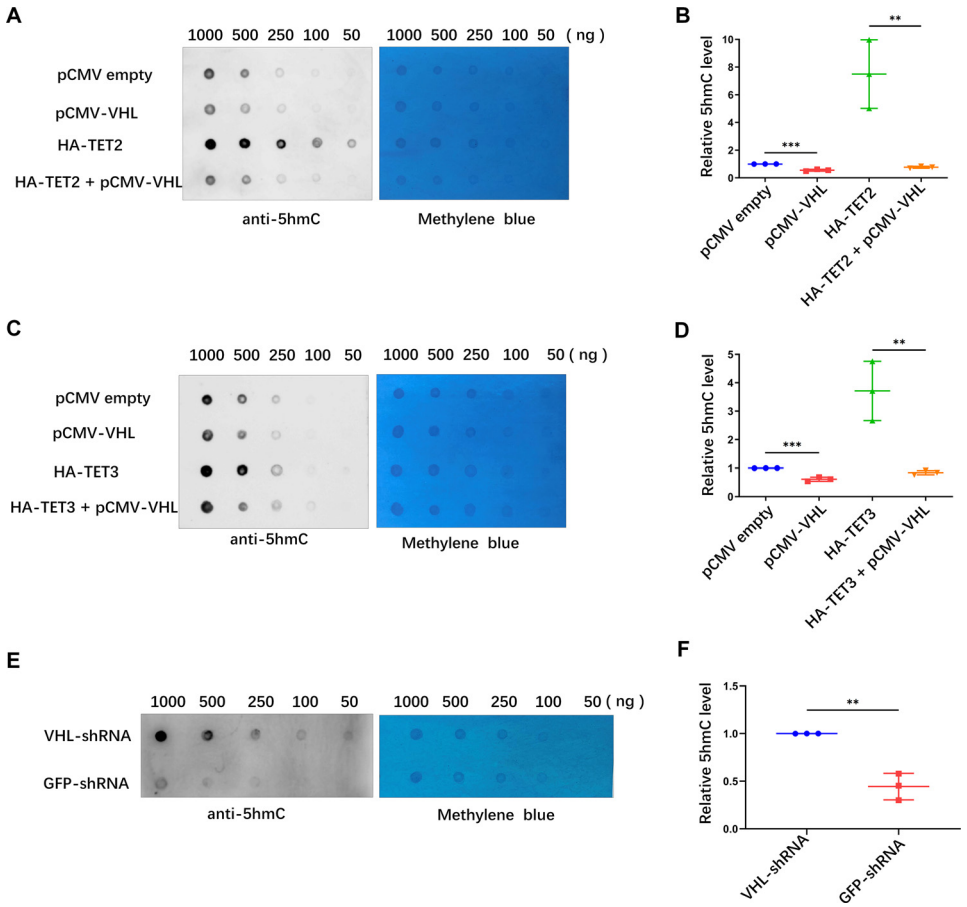

Figure 2. pVHL reduces globe 5hmC levels. *A*, dot blot analysis for 5hmC indicates that overexpression of pVHL causes TET2-induced 5hmC to diminish significantly in H1299 cells. *B*, quantitation of relative 5hmC levels in Fig. 1*A*. *C*, dot blot analysis for 5hmC indicates that overexpression of pVHL causes TET3-induced 5hmC diminished significantly in H1299 cells. *D*, Quantitation of relative 5hmC levels in Fig. 1*C*. *E*, the globe 5hmC levels were increased when pVHL was knocked down by pVHL-shRNA in H1299 cells. *F*, quantitation of relative 5hmC levels in Fig. 1*E*. Data are presented as mean ± S.D.; *$p < 0.05$, **$p < 0.01$, ***$p < 0.001$, ****$p < 0.0001$ (unpaired Student's *t* test); *ns*, no significance.

and PHD3 mutant (PHD3-mut) had no obvious effect on TET2/3 protein stability (Fig. 4, *A–D*). Furthermore, overexpression of WT, but not mutant PHD2 or PHD3, induced degradation of endogenous TET2/3 in H1299 cells (Fig. 4, *E* and *F*). To verify these results, we added the hydroxylase inhibitor DMOG (dimethyloxalylglycine) (53) to the cell culture medium, which enhanced the protein levels of TET2/3 and HIF-2α (positive control) in a dose-dependent manner (Fig. 4*G* and Fig. S5*A*). Furthermore, treatment with DMOG enhanced endogenous TET2/3 protein levels in mouse embryonic fibroblast (MEF) cells (Fig. 4*H*).

Collectively, these data suggest that PHD2/3 interact with TET2/3 to mediate TET protein degradation and that the degradation depends on the hydroxylase activity of PHD.

pVHL induces TET2/3 protein degradation, which is dependent of prolyl hydroxylation of TET2/3 catalyzed by PHD2/3

To verify that prolyl hydroxylation of TET proteins is required for pVHL-mediated degradation, we examined the effect of pVHL on the protein stability of TET2/3 with proline residues mutated in the LAP/LAP-like motifs. Compared with TET2-wt and TET3-wt, TET2-Pro/Ala (TET2-P1248A/P1255A) and TET3-Pro/Ala (TET3-P948A/P955A) mutants were less obviously degraded by coexpression of pVHL in HEK293T cells (Fig. 5, *A* and *B*). Of note, the LAP/LAP-like motifs are located in the core-catalytic domains (CD) of TET2 (amino acids 1030–1912) and TET3 (amino acids 837–1713), which are essential for the enzymatic activity of TET2/3 (54). However, the enzymatic activity of TET2/3 was not affected when proline was mutated to alanine, suggesting that proline residue might influence protein stability of TET2/3 but not enzymatic activity (Fig. S6). We sought to determine whether pVHL specifically induces degradation of the CD in TET2/3. Coexpression of pVHL caused a decrease in the protein levels of TET2-CD (amino acids 1030–1912) and TET3-CD (amino acids 837–1713) (Fig. S7, *A* and *B*). Moreover, coexpression of pVHL also did not induce degradation of TET2/3-CD mutants in which proline residues were mutated to alanine (TET2/3-CD-Pro/Ala) (Fig. S7, *A* and *B*).

To further confirm that pVHL mediates proteasomal degradation *via* the CD of TET2 or TET3, we performed ubiquitination assays with TET2/3-CD. MG132 was added to block proteasomal degradation of TET proteins by pVHL. As expected, coexpression of pVHL enhanced poly-ubiquitination of TET2/3-CD-wt but not TET2/3-CD-Pro/Ala (Fig. 5, *C* and *D*).

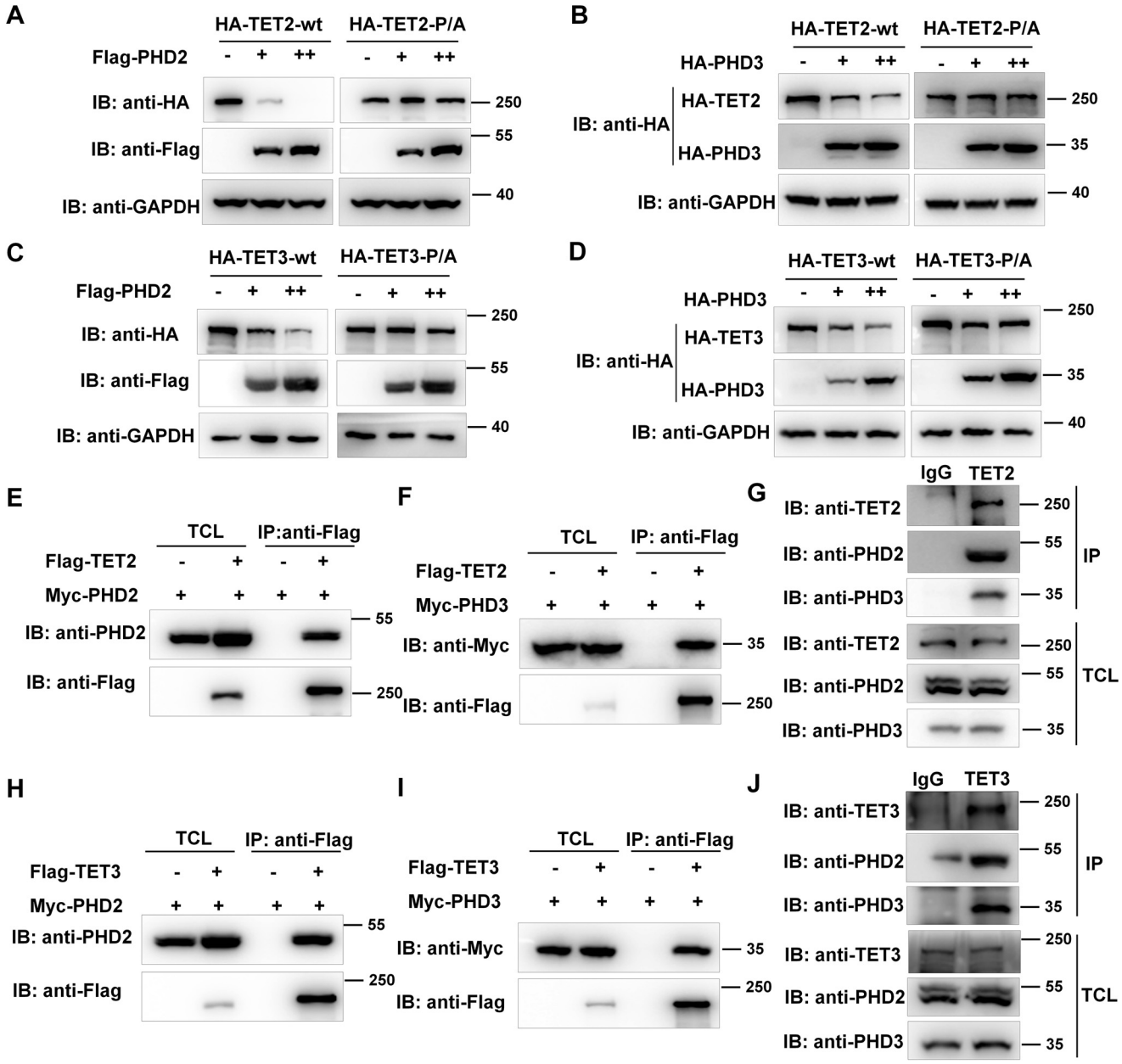

Figure 3. PHD2/3 induce TET2/3 degradation and interact with TET2/3. *A* and *B*, PHD2 and PHD3 induces degradation of WT TET2 (TET2-wt) but not of TET2-Pro/Ala mutant (TET2-P1248A/P1255A) in HEK293T cells. *C* and *D*, PHD2 and PHD3 induce degradation of WT TET3 (TET3-wt) but not of TET3-Pro/Ala mutant (TET3-P948A/P955A) in HEK293T cells. *E* and *F*, TET2 interacts with PHD2 or PHD3 in HEK293T cells revealed by co-immunoprecipitation assays. *G*, endogenous TET2 interacts with endogenous PHD2 or PHD3 revealed by co-immunoprecipitation assays in H1299 cells. Anti-TET2 antibody was used for co-immunoprecipitation, and rabbit IgG was used as control. *H* and *I*, TET3 interacts with PHD2 and PHD3 in HEK293T cells revealed by co-immunoprecipitation assays. *J*, endogenous TET3 interacts with endogenous PHD2 or PHD3 revealed by co-immunoprecipitation assays in H1299 cells. Anti-TET3 antibody was used for co-immunoprecipitation, and rabbit IgG was used as control. (*A–D*) *IB*, immunoblotting; (−), the cells transfected with the empty vector control; (+), the cells transfected with the indicted vector (0.5 μg); ($^{2+}$), the cells transfected with the indicated vector (1.0 μg). (*E–J*) *IB*, immunoblotting; *IP*, immunoprecipitation; *TCL*, total cell lysate; (−), the cells transfected with the empty vector control; (+), the cells transfected with the indicated vector.

Conversely, knockdown of pVHL by coexpression of pVHL-shRNA reduced the poly-ubiquitination of TET2/3-CD-wt (Fig. 5*E*).

To confirm that PHDs indeed catalyze TET prolyl hydroxylation, we developed specific antibodies against hydroxylated TET2 based on the proline residues located in the LAP/LAP-like motifs. The anti-hydroxylated-TET2 antibody (anti-TET2-OH) and anti-hydroxylated-TET3 antibody (anti-TET3-OH) worked well and were validated by dot blot assays (Fig. S8). As shown in Fig. 5*F*, overexpression of PHD3 enhanced hydroxylation of TET2-wt but not TET2-Pro/Ala. Moreover, MG132 treatment dramatically enhanced hydroxylation of endogenous TET2 (1.00 *versus* 2.83), but DMOG treatment reduced hydroxylation of endogenous TET2 (1.00 *versus* 0.56) (Fig. 5*G*). Notably, even though the enhancement effect of MG132 and DMOG on endogenous TET2 protein level was quite similar (1.55 *versus* 1.00; 1.48 *versus* 1.00), the ratio of hydroxylated TET2 in total TET2 of MG132 treatment was four times higher than that in DMOG treatment (2.83 *versus* 0.56) (Fig. 5*G*). This difference further indicated that MG132 blocked proteasomal

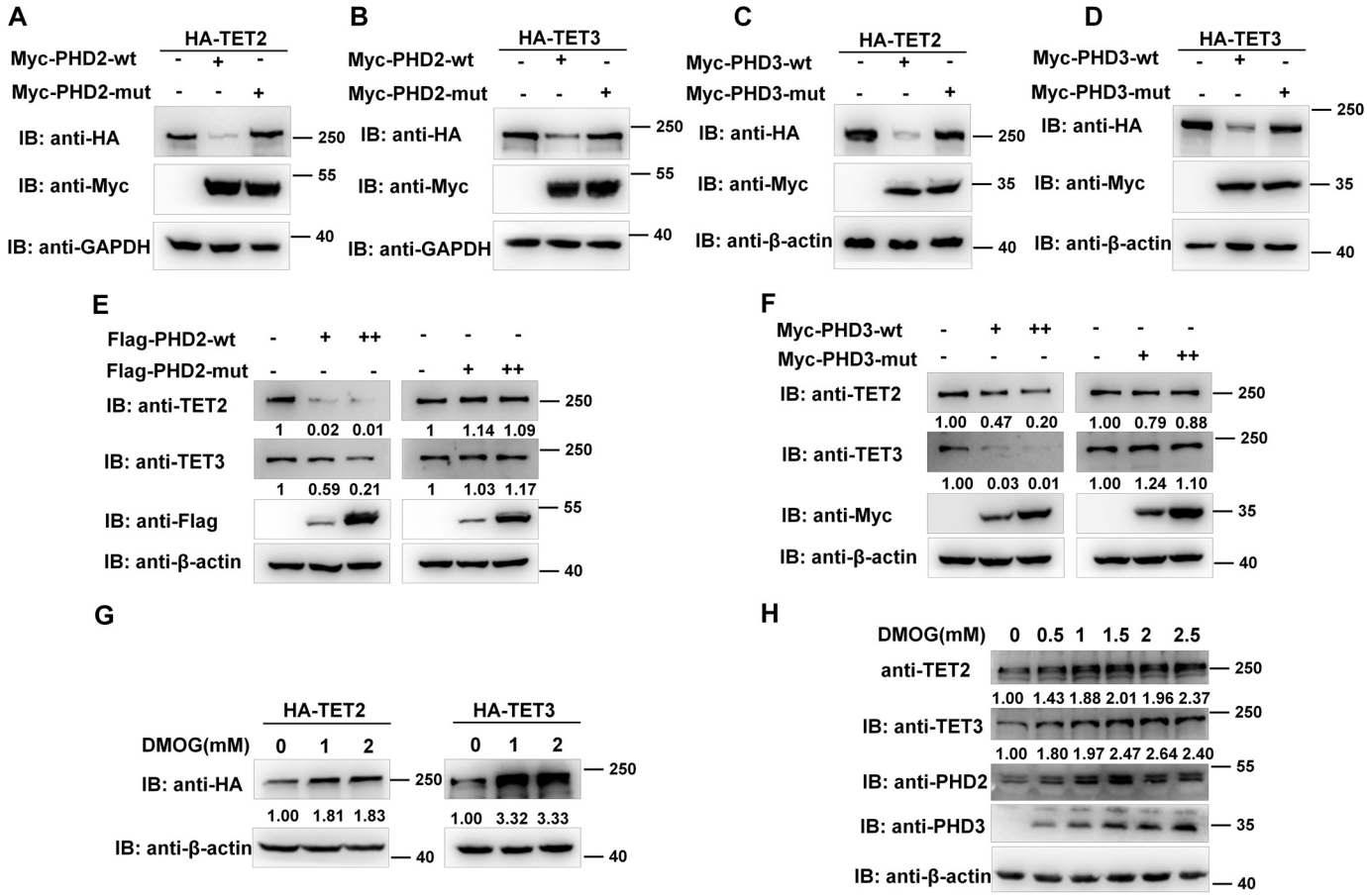

Figure 4. PHD2/3 induce degradation of TET2/3 depending on PHD proline hydroxylase activity. *A* and *B*, catalytically inactive PHD2-mut (PHD2-H290/351A) does not induce degradation of TET2 or TET3 in HEK293T cells. *C* and *D*, catalytically inactive PHD3-mut (PHD3-H135A/H196A) does not induce degradation of TET2 and TET3 in HEK293T cells. *E* and *F*, catalytically inactive PHD2-mut or catalytically inactive PHD3-mut does not induce degradation of endogenous TET2 and TET3 in H1299 cells. *G*, hydroxylase inhibitor DMOG enhances transfected HA-TET2 or HA-TET3 in HEK293T cells. *H*, DMOG enhances endogenous TET2 or TET3 in MEF cells. *IB*, immunoblotting; (−), the cells transfected with the empty vector control; (+), the cells transfected the indicted vector (0.5 μg); ($^{2+}$), the cells transfected with the indicated vector (1.0 μg).

degradation of hydroxylated TET2 but DMOG blocked hydroxylation of TET2, leading to a similar effect eventually, an enhancement of endogenous TET2 protein. Similar results were obtained by using anti-hydroxylated-TET3 antibody (anti-TET3-OH) (Fig. 5, *H* and *I*).

In addition, we synthesized six biotinylated hydroxylated or unhydroxylated peptides covering the predicted hydroxylated proline residues in HIF-1α (Pro-564) (used as a control), TET2 (Pro-1248/1255), and TET3 (Pro-948/955), respectively, and performed peptide pull-down assays (Fig. S9*A*) (11, 55). As shown in Fig. S9*B*, the biotinylated hydroxylated peptides of HIF-1α, TET2, or TET3 pulled down pVHL efficiently. By contrast, the biotinylated unhydroxylated peptides of HIF-1α, TET2, or TET3 could not pull down pVHL (Fig. S9*B*). Moreover, the N-terminal β domain deleted mutant of pVHL (Myc-VHL-Δ64–154) could not be pulled down by the biotinylated hydroxylated peptides of HIF-1α, TET2, or TET3 (Fig. S9*C*). On the contrary, the C-terminal β domain deleted mutant of pVHL (Myc-VHL-Δ193–204) could still be pulled down by the biotinylated hydroxylated peptides of HIF-1α, TET2, or TET3 (Fig. S9*C*). Taken together, these data suggest that prolyl hydroxylation mediates the effect of pVHL on TET degradation and the N-terminal β domain of pVHL is required for pVHL binding to hydroxylated TET.

Collectively, these data support a model in which pVHL induces TET2/3 proteasomal degradation and prolyl hydroxylation of TET2/3 catalyzed by PHD2/3 is required for this process.

TET2/3 could rescue hypoxia-induced hypermethylation

It has been reported that hypoxia causes DNA hypermethylation by reducing TET activity (15, 19). We noticed that TET2 but not TET3 was induced under hypoxia in H1299 cells (Fig. S10*A*). In addition, under hypoxia, the global 5hmC levels were reduced in H1299 cells (Fig. S10*B*). However, overexpression of TET2/TET3 could rescue hypoxia-induced reduction of global 5hmC levels (Fig.S10*B*), further suggesting an important role of TET2/3 in hypoxia-induced DNA hypermethylation.

Comparison of pVHL-mediated degradation on HIF-α proteins and TET proteins

It has been well-established that pVHL mediates HIF-1α and HIF-2α proteasomal degradation depending on the prolyl

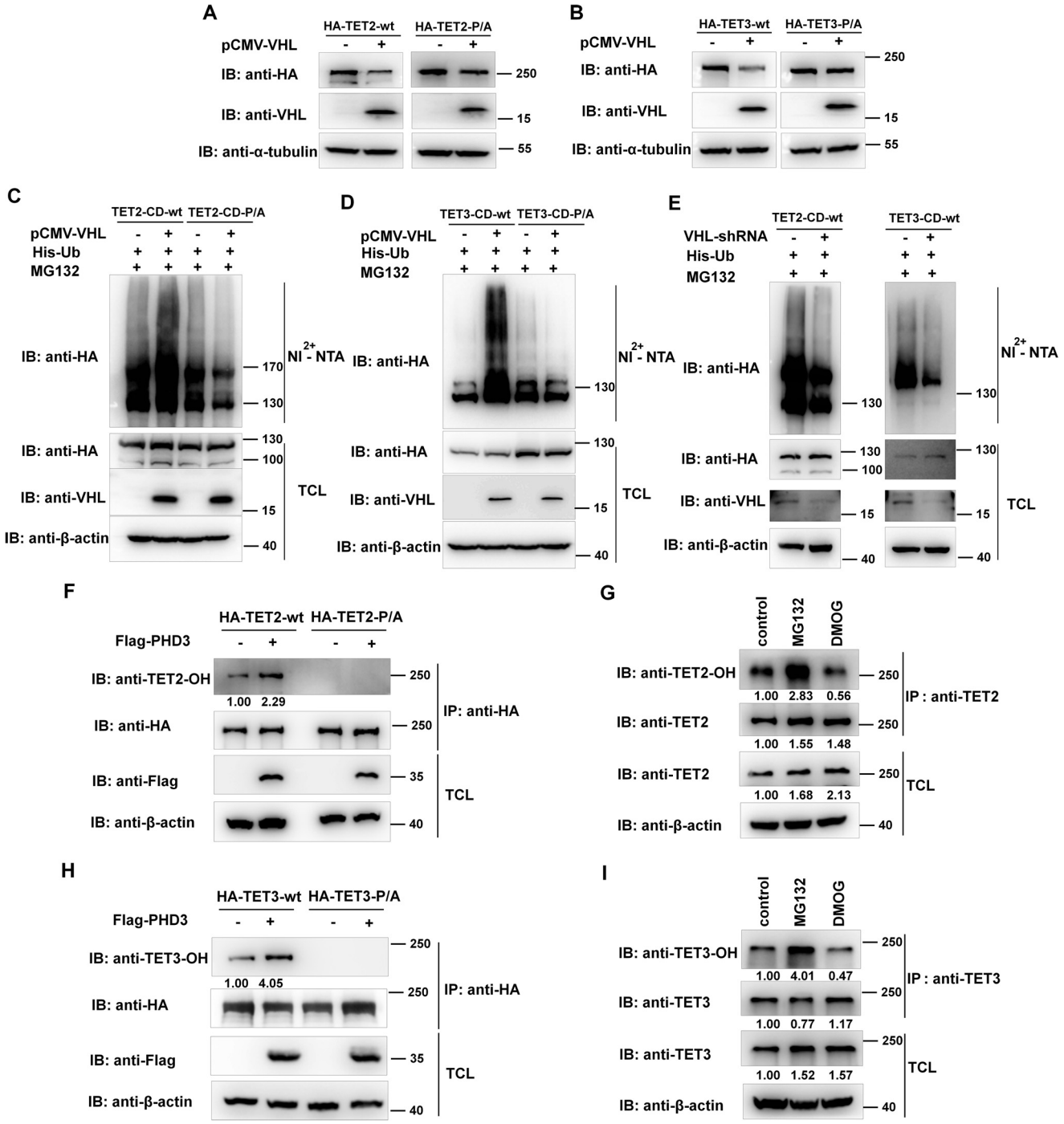

Figure 5. pVHL and PHD3 induce poly-ubiquitination of TET2/3 depending on HIF-ODD-like/LAP motif in TET2/3. *A* and *B*, overexpression of pVHL induces degradation of WT TET2 and TET3 but causes TET2-Pro/Ala mutant and TET3-Pro/Ala mutant to be barely diminished. *C*, pVHL catalyzes poly-ubiquitination of WT TET2-CD (TET2-CD-wt) but not of TET2-CD-Pro/Ala mutant. *D*, pVHL catalyzes poly-ubiquitination of WT TET3-CD (TET3-CD-wt) but not of TET3-CD-Pro/Ala mutant. *E*, knockdown of pVHL by pSuper-VHL-shRNA causes reduction of poly-ubiquitination of WT TET2-CD (TET2-CD-wt) or WT TET3-CD (TET3-CD-wt) in H1299 cells. *F*, overexpression of PHD3 enhances hydroxylation of WT TET2 (TET2-wt) but not of TET2-Pro/Ala mutant as revealed by anti-TET2-OH antibody. HEK293T cells were transfected with the indicated plasmids. After co-immunoprecipitation using anti-HA conjugated agarose beads, the loading amount of protein was adjusted to similar levels between the samples with and without PHD3 overexpression based on the pilot experiments. *G*, the proteasomal inhibitor MG132 causes enhancement of hydroxylation of TET2 and the hydroxylase inhibitor DMOG causes reduction of hydroxylation of TET2. MG132 (20 μM) or DMOG (1 mM) was added to the culture medium for 8 h before cells were harvested; DMSO was used as a carrier control. *C–E*, HEK293T or H1299 cells were transfected with the indicated vectors; MG132 (20 μM) was added to the culture medium; the cell lysates underwent affinity purification using nickel-nitrilotriacetic acid resin; and anti-HA was used for detection. *IB*, immunoblotting; *TCL*, total cell lysate; (−), the cells transfected with the empty vector control; (+), the cells transfected with the indicated vector.

hydroxylation catalyzed by PHDs. PHDs are thought to serve as oxygen sensors (40). Therefore, we speculated that the effect of pVHL on TET may also be similarly affected by the oxygen status. To explore this possibility, we first established a system for assessing hypoxia effects by cotransfecting VHL together with FLAG-HIF-1α or FLAG-HIF-2α in HEK293T cells. Under

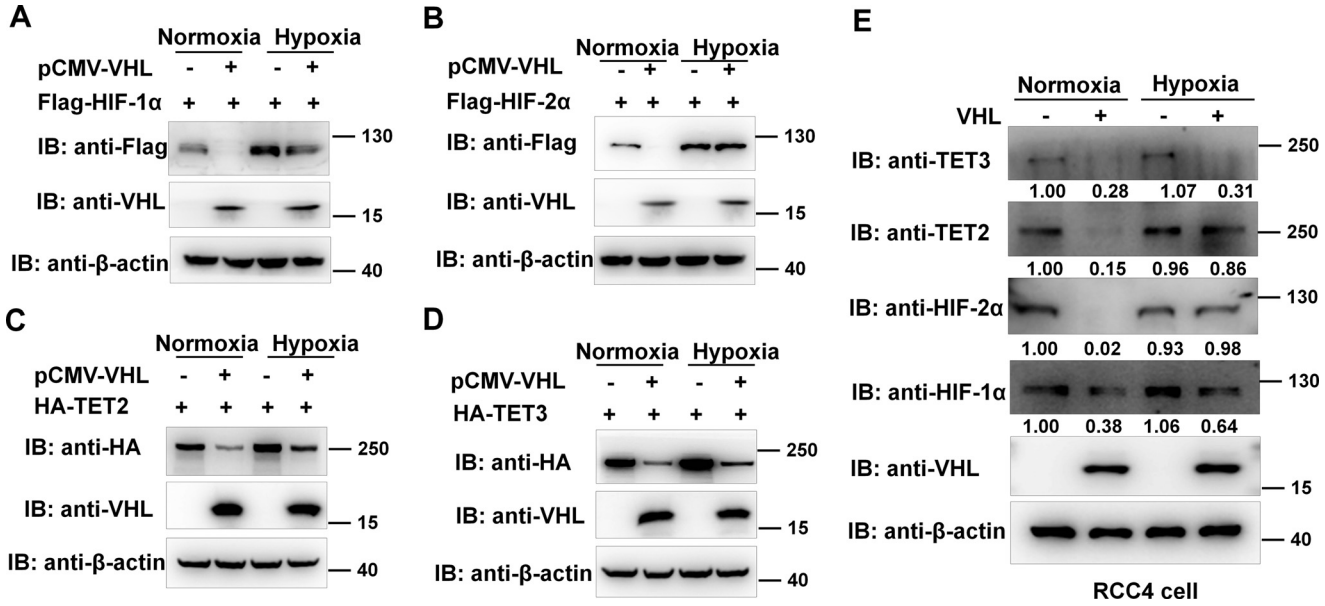

Figure 6. Comparison of TET2 and TET3 with HIF-1α and HIF-2α degradation induced by pVHL. *A*, pVHL induces degradation of overexpressed HIF-1α under normoxia, which is partially recovered under hypoxia (2% O_2) in HEK293T cells. *B*, pVHL induces degradation of overexpressed HIF-2α under normoxia, which is recovered under hypoxia (2% O_2) in HEK293T cells. *C*, pVHL induces degradation of overexpressed TET2 under normoxia, which is partially recovered under hypoxia (2% O_2) in HEK293T cells. *D*, pVHL induces degradation of overexpressed TET3 under normoxia and hypoxia (2% O_2) in HEK293T cells. *E*, comparison of endogenous TET3, TET2, HIF-2α, and HIF-1α in parental RCC4 cells (−) or RCC4 cells reconstituted with pVHL (+) under normoxia and hypoxia. *A–D*, HEK293T cells were transfected with the indicated plasmids. After transfection for 10–12 h, the cells were subjected for hypoxia treatment for 10–12 h (2% O_2) or kept in normoxic conditions (21% O_2). Then, the cells were harvested for Western blotting analysis. *IB*, immunoblotting; *IP*, immunoprecipitation; *TCL*, total cell lysate; (−), the cells transfected with the empty vector control; (+), the cells transfected with the indicated vector.

normoxia (21% O_2), coexpression of VHL significantly reduced protein levels of both FLAG-HIF-1α and FLAG-HIF-2α, as expected, whereas under hypoxia (2% O_2), coexpression of pVHL had no effect on HIF-2α (Fig. 6, *A* and *B*). Intriguingly, under hypoxia, coexpression of pVHL still reduced HIF-1α protein levels, which might suggest that the hydroxylation of HIF-1α by PHDs is more sensitive than the hydroxylation of HIF-2α by PHDs. This phenomenon might also reflect differences in the behaviors and functions of HIF-1α and HIF-2α in the hypoxia signaling pathway (4).

Next, we cotransfected VHL together with HA-TET2/3. Under normoxia, pVHL caused obvious decrease in TET2/3, whereas under hypoxia, pVHL still caused decreases, but they were less dramatic than under normoxia, which is similar to what was observed for HIF-1α (Fig. 6, *C* and *D*).

To compare the effect of pVHL on endogenous HIF-1α, HIF-2α, TET2, and TET3, we used RCC4 cells, a VHL-deficient kidney cancer cell line in which HIF-α (HIF-1α and HIF-2α) is highly expressed under normoxia (56). Similar to cotransfection assay results, reconstitution of pVHL in RCC4 cells caused a reduction of HIF-1α, HIF-2α, TET2, and TET3 under normoxia. Under hypoxia, similar levels of HIF-2α and TET2 were observed with/without VHL but HIF-1α was reduced somewhat and TET3 was reduced dramatically (Fig. 6*E*). In addition, the TET2 and TET3 mRNA levels were lower in parental RCC4 cells compared with those in RCC4 cells reconstituted with VHL (RCC4/VHL) under normoxia (Fig. S11*A*), which indicated that pVHL did not affect TET expression via HIF-dependent transactivation, different from that in H1299 cells. Therefore, the effect of pVHL on TET proteins appears to be the most similar to the effect of pVHL on HIF-α. Of note, the global 5hmC levels were lower in RCC4/VHL cells compared with parental RCC4 cells under normoxia (Fig. S11, *B* and C). Interestingly, under hypoxia, the global 5hmC levels were still lower in RCC4/VHL cells compared with RCC4 cells (Fig. S11, *B* and *C*), implicating that pVHL might still have an effect on TET2/3 function even under hypoxia.

Therefore, the mechanism of pVHL-mediated TET proteasomal degradation is similar to that of pVHL-mediated HIF-α proteasomal degradation.

Zebrafish vhl, egln1a(phd2a), egln1b (phd2b), and egln3 (phd3) mediate reduction of global 5hmC levels in vivo

Zebrafish *vhl* and *tet* enzymes have functions similar to their orthologs in mammalians (Fig. S12) (57, 58). To gain insight into the physiological role of pVHL and PHDs on the stability of TET proteins and their global 5hmC levels, we took advantage of the zebrafish models. As for mammalian pVHL, zebrafish vhl induced zebrafish tet2-CD (amino acids 883–1715) and tet3 degradation when *vhl* was overexpressed in HEK293T cells (Fig. 7, *A* and *B*). To confirm the role of *vhl* on global 5hmC levels *in vivo*, we injected synthetic *vhl* mRNA or GFP mRNA control into zebrafish embryos at the one-cell stage. After 24 h, the embryos were harvested for dot blot assays by anti-5hmC antibody. The global 5hmC levels were significantly decreased in embryos injected with *vhl* mRNA compared with those injected with GFP mRNA control (Fig. 7, *C* and *D*). Expression of injected mRNA was confirmed by Western blotting analysis (Fig. 7*E*). Consistently, the global 5hmC levels were enhanced significantly in *vhl*-null zebrafish larvae ($vhl^{-/-}$) (6 dpf)

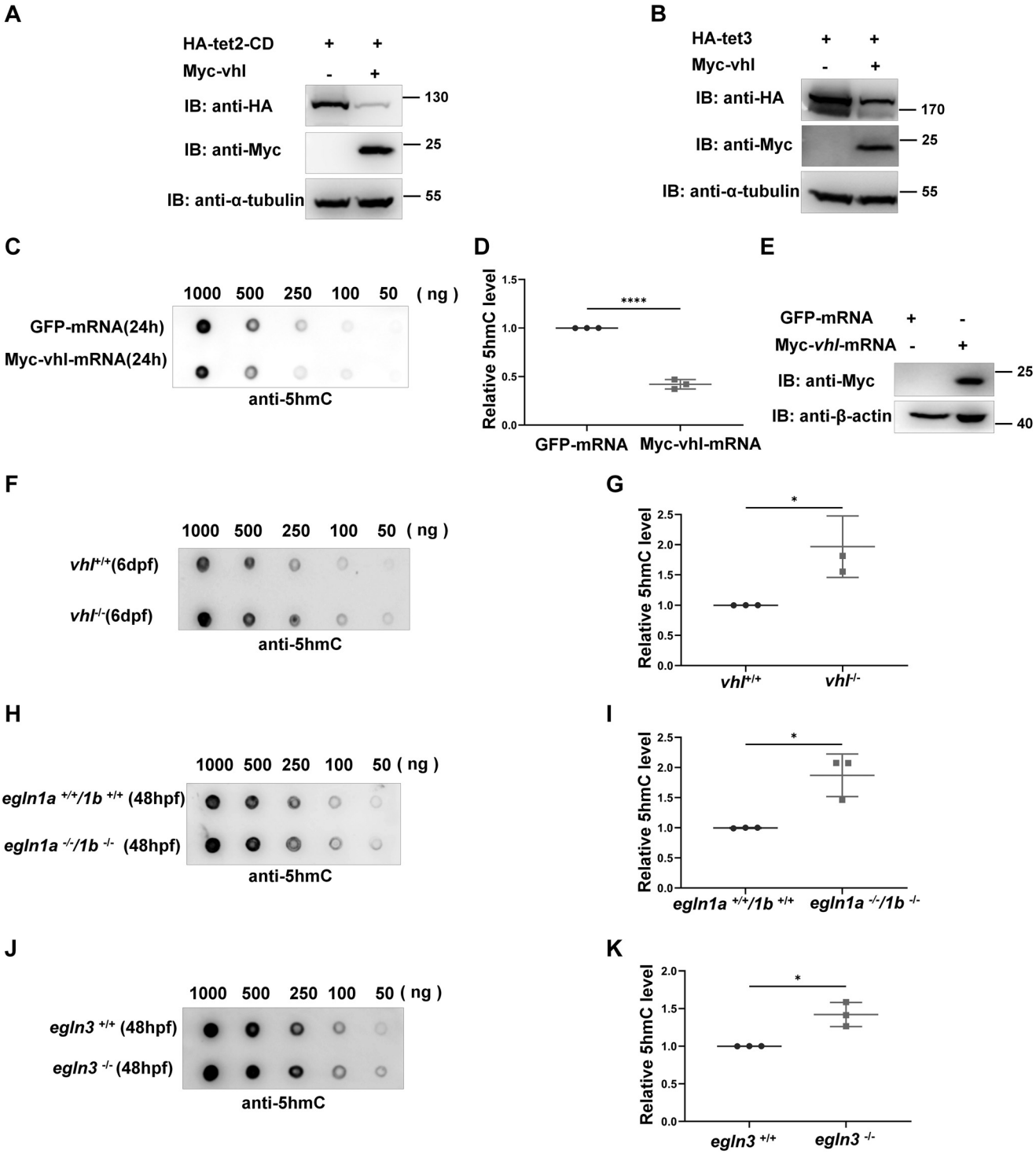

Figure 7. Zebrafish *vhl*, *egln1a/b*, and *egln3* reduce global 5hmC levels *in vivo*. *A* and *B*, zebrafish vhl induces degradation of zebrafish tet2-CD (aa 883–1715) and tet3 in HEK293T cells. HEK293T cells were transfected with the indicated plasmids. After transfection for 24 h, the cells were harvested and the proteins were detected by Western blotting analysis. *C*, dot blot analysis for 5hmC indicates that global 5hmC levels in the embryos injected with *vhl* mRNA ($n = 50$ each group) is diminished significantly compared with the embryos injected with GFP mRNA control (24 h) ($n = 50$ in each group). *D*, quantitation of Fig. 7*C*. *E*, expression of injected *vhl* mRNA is confirmed by Western blotting analysis. *F*, the global 5hmC levels in *vhl*-null zebrafish larvae ($vhl^{-/-}$) (6dpf, $n = 50$ each group) are enhanced significantly compared with the WT controls ($vhl^{+/+}$) (6dpf, $n = 50$ each group). *G*, quantitation of Fig. 7*F*. *H*, the global 5hmC levels in *egln1a/1b*-double-null zebrafish embryos ($egln1a^{-/-}/egln1b^{-/-}$) (48 hpf, $n = 50$ each group) compared with the WT embryos (48 hpf, $n = 50$ in each group). *I*, quantitation of Fig. 7*H*. *J*, the global 5hmC levels in *egln3* null zebrafish embryos ($egln3^{-/-}$) (48 hpf, $n = 50$ in each group) compared with the WT embryos (48 hpf, $n = 50$ each group). *K*, quantitation of Fig. 7*J*. *IB*, immunoblotting; (−), the cells transfected with the empty vector control; (+), the cells transfected with the indicated vector. Data are presented as mean ± S.D.; $*p < 0.05$, $**p < 0.01$, $***p < 0.001$, $****p < 0.0001$ (unpaired Student's *t* test).

compared with WT control larvae ($vhl^{+/+}$) (6 dpf) (Fig. 7, *F* and *G*). These data suggest that *vhl* reduces global 5-mhC levels *in vivo* by targeting tet for degradation.

Subsequently, we sought to determine whether zebrafish *egln*s (*phd*s) are also involved in *vhl* function in reducing tet enzymatic activity *in vivo*. Zebrafish have two *egln1* (*phd2*) genes, *egln1a* (*phd2a*) and *egln1b* (*phd2b*), both of which are evolutionarily conserved with mammalian PHD2 (EGLN1) (Fig. S13), and an *egln3* (*phd3*) gene, which is also evolutionarily conserved with mammalian PHD3 (EGLN3) (Fig. S14). Furthermore, zebrafish *egln1a* (*phd2a*), *egln1b* (*phd2b*), and *egln3* could induce degradation of zebrafish tet2-CD and tet3, as well (Fig. S15).

To further characterize the physiological role of *egln1a, egln1b*, and *egln3* in regulating 5hmC levels *in vivo*, we generated *egln1a*-null, *egln1b*-null, and *egln3*-null zebrafish, respectively, by CRISPR/Cas9 techniques (Fig. S16). Through cross-breeding, we also obtained *egln1a/egln1b* double-null zebrafish ($egln1a^{-/-}/egln1b^{-/-}$) and *egln3*-null zebrafish ($egln3^{-/-}$). Overall, these homozygous zebrafish were physiologically indistinguishable from their WT siblings. By dot blot assays, the global 5-hmC levels in $egln1a^{-/-}/egln1b^{-/-}$ embryos were higher than those in WT control embryos (Fig. 7, *H* and *I*). Similarly, the global 5-hmC levels in $egln3^{-/-}$ embryos were higher than those in WT control embryos (Fig. 7, *J* and *K*). These data suggest that zebrafish *egln*s (*phd*s) mediate *vhl*'s function in reducing tet enzymatic activity *in vivo*.

To determine whether the role of *vhl*, *egln1a*, *egln1b*, and *egln3* in regulating 5hmC levels *in vivo* is dependent of HIF-α, we used 2ME2 (150 μM) to block HIF-α function and examined global 5-hmC levels. Initially, we examined the *tet2* and *tet3* mRNA levels in zebrafish embryos with different genetic backgrounds. Similar to what was exhibited in the VHL-knockdown H1299 cell line, the mRNA levels of *tet2* and *tet3* and of *vegfa* (positive control) were increased in *vhl*-null zebrafish (6 dpf) compared with those in the WT siblings (6 dpf), further suggesting that *vhl* can regulate expression of *tet2/3* at the transcriptional level (Fig. S17*A*). However, the mRNA levels of *tet2/3* and of *vegfa* were not altered in *egln1a/egln1b* double-null embryos (48 hpf) compared with those in the WT siblings (48 hpf), indicating that *egln1* does not modulate expression of *tet2/3* at the transcriptional level (Fig. S17*B*). Similar to what was exhibited in *vhl*-null zebrafish, the mRNA levels of *tet2/3* and of *vegfa* were increased in *egln3*-null zebrafish (48 dpf) compared with those in the WT siblings (48 dpf), suggesting that *egln3* might also regulate expression of *tet2/3* at the transcriptional level (Fig. S17*C*). Given the increasing of *tet2/3* expression in *vhl*-null and *egln3*-null zebrafish, to clarify whether the increasing of global 5-hmC levels exhibited in *vhl*-null and *egln3*-null zebrafish is dependent of the HIF pathway, we used 2ME2 (150 μM) to block HIF function in zebrafish larvae or embryos. Treatment with 2ME2 decreased the mRNA levels of *tet2/3* and of *vegfa* significantly in *vhl*-null zebrafish (Fig. S17*D*), suggesting that 2ME2 can effectively block HIF-α function in zebrafish larvae and embryos. However, as shown in Fig. S17, *E* and *F*, the global 5-hmC levels were still higher in *vhl*-null zebrafish compared with their WT siblings. Similarly, the global 5-hmC levels were also higher in *egln3*-null zebrafish compared with their WT siblings (Fig. S17, *G–I*). These data indicate that the role of *vhl* and *egln3* in regulating 5hmC levels *in vivo* is independent of HIF-α.

Collectively, these data suggest that zebrafish *vhl*, *egln1a/b (phd2)*, and *egln3 (phd3)* have functions similar to those in mammalians in causing the reduction of global 5hmC levels by mediating tet degradation, which seems to be independent of the HIF pathway.

Discussion

Global DNA hypomethylation and promoter-specific hypermethylation are hallmarks of most cancers (59, 60). Global hypomethylation promotes genomic instability and cell transformation (61). In particular, it has been reported that global DNA hypomethylation is also a feature of kidney cancer (62, 63). As a key tumor suppressor gene for kidney cancer, pVHL has been assessed for its role in genome methylation, though the results are controversial (64, 65). Through systematic DNA methylation analysis using prototypical ccRCC cell lines (RCC4 and 786-O), which are VHL-deficient, Ohh and co-workers (65) have provided evidence to show that gain of pVHL results in global DNA hypermethylation. These observations are consistent with the observation that global hypomethylation is common in kidney cancer, particularly in VHL mutated ccRCC (62, 63). However, the mechanism underlying this phenomenon is largely unknown. Here, we determined that pVHL induces TET proteasomal degradation *in vitro* and *in vivo*, resulting in increased global 5-hmC levels. These findings might explain, at least in part, why global hypomethylation is commonly observed in ccRCC.

Because the prolyl hydroxylation of hypoxia-induced factors (HIF-1α and HIF-2α) is catalyzed by EGLNs (PHDs) under normoxia and is prerequisite for subsequent pVHL-mediated proteasomal degradation, the PHD-pVHL pathway is thought to be a major mechanism underlying the functions of HIF-1α and HIF-2α in the hypoxia signaling pathway (66–69). Multiple additional targets of either VHL or PHDs, or both, have been identified; however, the mechanism similar to that of VHL and PHDs in regulating HIF-1α and HIF-2α has not been elucidated. In most of the cases, prolyl hydroxylation is not required for pVHL-mediated degradation or inhibition of pVHL's targets (5–7, 9, 10). Though PHD2-mediated AKT proline-hydroxylation is required for pVHL to suppress AKT kinase activity, pVHL does not induce AKT proteasomal degradation (11). ZHX2 has been identified as a VHL target, and its hydroxylation allows VHL to regulate its protein stability, but PHDs do not appear to be involved in ZHX2 hydroxylation (12). In addition, specific targets of PHDs have been identified that are modulated by PHD-catalyzed hydroxylation, but pVHL is not involved (70–72). In this study, we identified TET proteins as pVHL's targets and demonstrated that PHD2/PHD3-mediated prolyl hydroxylation is required for pVHL-induced proteasomal degradation, which is similar to the mechanism by which PHD-pVHL regulates HIF-α and further extends the role of the PHD-pVHL pathway, reinforcing the importance of this unique system for regulating protein stability. Notably, the pattern of

PHD-pVHL-mediated TET degradation might not be exactly the same as that of PHD-pVHL on HIF-α. Our results suggest that the activity of PHD-pVHL on TET2 is very close to that of PHD-pVHL on HIF-α, but for TET3, the activity of PHD2 or PHD3 is high enough to catalyze TET3 at very low levels of oxygen, even under hypoxia (2% O_2). In fact, the PHDs enzymatic activity has been shown to differ under similar oxygen concentrations for different substrates, such as HIF-1α and HIF-2α (29, 73) (this study). Importantly, we provide evidence to show that the prolyl hydroxylation is prerequisite for pVHL-mediated TET proteasomal degradation, which suggests a fundamental similarity in the mechanism of TET and HIF-α. Even though the regulation of TET protein stability has been investigated, the reports about degradation of TET protein through a classic ubiquitin-proteasome system are rare. Here, we reveal degradation of TET proteins through the ubiquitin-proteasome system, opening a new window for understanding the regulation of TET stability and global DNA demethylation.

In addition to reducing TET activity, hypoxia has also been shown to enhance TET expression via HIF-dependent transactivation of TET1/2/3, even though some data are inconsistent (15, 19–21, 28, 41). Given a key regulator of HIF-α, pVHL might also modulate TET expression via HIF-dependent transcription. In fact, in this study, we showed that pVHL could affect TET transcription depending on HIF-α in H1299 cells. However, to what extent this modulation contributes to TET function is still difficult to distinguish. As observed in this study, it seemed that the global 5hmC levels were not correlated with *TET* mRNA levels. However, we provided multiple lines of evidence to show that pVHL could modulate TET protein stability independent of HIF, resulting in changes of global 5hmC levels. These data suggest that pVHL can regulate TET at both the transcriptional level and the protein level under certain conditions but that pVHL might mainly act its role on TET function via modulation of TET at the protein level, which is independent of the HIF pathway. In zebrafish, similar to *vhl*, *phd3* could modulate *tet* expression via HIF-dependent transcription, but *phd3* could also affect global 5hmC levels independent of the HIF pathway.

Although divergent functions have been reported among TET1, TET2, and TET3 (27), all TET proteins are thought to have critical roles in regulating DNA methylation patterns. Because of a lack of functional antibody against TET1, we did not analyze the regulation of TET1 by pVHL in detail. However, based on the conserved structure of TET proteins and the data obtained in this study, pVHL might have a role in modulating TET1 that is similar to its role in modulating TET2 and TET3, with PHD2 and PHD3 as key contributing factors.

In summary, we identified TET proteins as substrates of pVHL. Similar to HIF-α proteins, the prolyl hydroxylation of TET proteins catalyzed by PHD2/3 is prerequisite for pVHL-mediated proteasomal degradation. These observations not only extend our knowledge about regulation of DNA methylation through posttranslational modification of TET proteins but also help provide insight into the mechanisms of pVHL in tumor suppression.

Experimental procedures

Plasmid constructs and mutants

The original WT mouse *Tet1*, *Tet2*, and *Tet3* were kindly provided by Guoliang Xu, and their truncated mutants were constructed by PCR and cloned into the indicated expression vectors. Mouse *PHD1*, *PHD2*, *PHD3*, *VHL*, and zebrafish *tet2*, *tet3*, *vhl*, *egln1a*, *egln1b*, *egln3*, and their mutants were constructed by RT-PCR and cloned into indicated expression vectors. pSuper-VHL-shRNA has been described previously (10). The target sequence of pSuper-VHL-shRNA is 5-GCCTGAGAATTACAGGAGA-3 (9, 10). pCMV-VHL was constructed by cloning mouse *Vhl* into pCMV-Myc vector (Clontech) at first, then removing the Myc tag (pCMV-VHL) or replacing it with a FLAG tag (FLAG-VHL). Because Myc-tagged mouse Vhl is close to the IgG band, which was difficult for immunoprecipitation assays, we cloned human *VHL* into pCMV-Myc vector (Myc-VHL) for immunoprecipitation assays.

Cell culture and transfection

HEK293T and H1299 cell lines were originally obtained from ATCC. RCC4 and RCC4-VHL cells were kindly provided by Peter J. Ratcliffe. They were maintained in DMEM (Biological Industries) supplemented with 10% FBS (Biological Industries) at 37 °C in a humidified atmosphere incubator containing 5% CO_2. All cell lines were verified to be free of *mycoplasma* contamination before using. VigoFect (Vigorous Biotechnology, Beijing, China) was used for cell transfection. MEF cells were established as described previously (74).

Antibodies and Western blotting analysis

The antibodies used were as follows: anti-FLAG antibody (F1804; 1:1000; Sigma-Aldrich), anti-c-Myc antibody (9E10; 1:1000; Santa Cruz), anti-HA antibody(1:5000; Covance), anti-GAPDH antibody (SC-47724; 1:1000; Santa Cruz), anti-β-actin (sc-47778; 1:2000; Santa Cruz), anti-α-tubulin antibody (EPR1333; 1:10000; Epitomics), anti-pVHL (1:500; ABclonal), anti-TET2 antibody (ab94580; 1:500; Abcam), anti-TET3 (ab139805; 1:500; Abcam), anti-PHD2 (catalog no. 4835; 1:500; Cell Signaling Technology), anti-PHD3(ab184714; 1:500; Abcam), anti-HIF-2α antibody (ab199; 1:500; Abcam), and anti-HIF-1α antibody (A6265; 1:500; ABclonal). Anti-TET2-OH antibody was raised against peptide TVIAP (OH) IYKKLAP (OH) DAY (Proteingene Technology, Wuhan, China). Anti-TET3-OH antibody was raised against peptide DLATEVAP (OH) LYKRLAP (OH) QAYQNQ (Proteingene Technology, Wuhan, China). Western blotting analysis was performed as described previously (74). The Fuji Film LAS4000 mini luminescent image analyzer was used for photographing the blots. Image-Pro Plus and Multi Gauge V3.0 were used for quantifying the protein levels based on the band density obtained in Western blotting analysis.

Quantitative analysis of global 5hmC levels by dot blot assays

H1299 cells, zebrafish embryos, or larvae were digested with Proteinase K (400 μg/ml, Roche) in STE buffer (0.2% SDS, 5 mM EDTA, 100 mM Tris-HCl, pH 8.5, and 200 mM NaCl) overnight at 55 °C. Next, genomic DNA was isolated using a standard phenol/chloroform extraction method. Genomic DNA was vacuum-dried and recovered in 10 mM Tris-HCl, pH 8.0. After sonication into ~500 bp fragments, the DNA was denatured with 0.1 M NaOH and 10 mM EDTA at 95 °C for 10 min, then placed on ice and neutralized with an equal volume of 2 M ammonium acetate, pH 7.0. Nitrocellulose membranes were washed in 2× SSC buffer, air-dried, and incubated in 2× SSC buffer at 37 °C for 15 min. The DNA samples were spotted onto the nitrocellulose membranes using a Bio-Dot apparatus (Bio-Rad). For DNA cross-linking, the membranes were washed with 2× SSC buffer, air-dried, and incubated at 80 °C for 2 h. Subsequently, the membranes were blocked with 5% nonfat milk for 2 h and incubated with anti-5hmC (catalog no. 39769; 1:1000; Active Motif) overnight at 4 °C. After washing three times in 5% nonfat milk, the membranes were incubated with HRP-conjugated secondary antibody for 1 h. The membranes were then washed for three times with 5% nonfat milk and once with TBS, and were visualized using an enhanced chemiluminescence detection kit (Millipore). A Fuji Film LAS4000 mini luminescent image analyzer was used for photographing the blots.

For quantification of relative 5hmC levels in dot blots, we used Image-Pro Plus software (Media Cybernetics). Briefly, the value of dot density in each control was treated as around 1.00, and the value of each control's corresponding dot was calculated by dividing the density of the corresponding dot with its control's density.

Immunofluorescent image for 5hmC

Immunofluorescent staining of 5hmC was performed as described previously with some modifications (75). Briefly, the cells were plated onto cover slips. After 48 h, the cells were fixed with 4% paraformaldehyde solution for 15 min at room temperature and then washed with PBS. For permeabilization, the cells were incubated with 0.5% Triton X-100 in PBS for 15 min at room temperature. To denature DNA, the cells were incubated with 4 M HCl for 20 min at room temperature, then rinsed with distilled water, and placed in 100 mM Tris-HCl, pH 8.5, for 10 min. After washing with PBS with Tween (PBST), nonspecific binding was blocked with blocking buffer (5% FBS, 0.1% Triton X-100, and 2 mg/ml BSA in PBS) for 1 h at room temperature. Then, the cells were incubated with anti-5hmC antibody at 1:500 in PBS solution containing 5% FBS, 0.1% Triton X-100, and 2 mg/ml BSA overnight at 4 °C. After washing with PBST, the cells were incubated with secondary antibody (Alexa Fluor 488 goat anti-rabbit IgG, catalog no. A11008) diluted at 1:300 in PBS solution containing 5% FBS, 0.1% Triton X-100, and 2 mg/ml BSA for 1 h at room temperature. The nuclei were counterstained with 4′,6-diamidino-2-phenylindole (1 mg/ml) for 30 min at room temperature. After a final washing with PBST, the stained cells were mounted with a mounting medium (catalog no. S36967, Thermo Fisher Scientific). The images were photographed under a laser confocal micro-imaging system. Image-Pro Plus software (Media Cybernetics) was used for quantifying the relative 5hmC levels based on immunostaining density.

In vivo ubiquitination assays

HEK293T cells were cotransfected with the indicated plasmids using VigoFect. Before harvesting, the cells were treated with MG132 (20 μM) (Calbiochem) for 8 h. The cell extracts were incubated with nickel-nitrilotriacetic acid beads (Novagen) for 12 h and then examined by Western blotting analysis using anti-HA antibody for detecting poly-ubiquitination of TET2 or TET3, respectively.

Quantitative real-time PCR analysis

The total RNA was extracted from cells using the Trizol reagent (Invitrogen), and the cDNA was synthesized using a First Strand cDNA Synthesis Kit (Fermentas). The primers used for RT-PCR analysis are listed in Table S1.

Generation of egln1a/egln1b double-null and egln3-null zebrafish

Zebrafish *egln1a*, *egln1b*, and *egln3* sgRNA were designed using a website tool (http://crispr.mit.edu). The zebrafish Codon Optimized Cas9 plasmid was digested with XbaI and purified and transcribed using the T7 mMessage mMachine Kit (Ambion). The PUC9 gRNA vector was used for amplifying the sgRNA template. The target sites for amplifying gRNA are *egln1a*: 5′-GGATAAAATCACCTGGATTGAG-3′; *egln1b*: 5′-GGTCGGACGCAGTATTCTGGAGG-3′; and *egln3*: 5′-GGACACGCAGTTGGAGAGTTTGG-3′. sgRNA was synthesized using the Transcript Aid T7 High Yield Transcription Kit (Fermentas). The zebrafish (*Danio rerio*) strain AB was raised, maintained, reproduced, and staged according to standard protocol. DNA (Cas9) and mRNA were injected into embryos at the one-cell stage. Cas9 RNA and sgRNA were injected at 0.75–1.25 ng/embryo and 0.075 ng/embryo, respectively. The mutations were initially detected by heteroduplex mobility assay as previously described (76). If the results were positive, the remaining embryos were raised up to adulthood as the F0, which were backcrossed with wild-type zebrafish (AB line) to generate the F1, which were genotyped by heteroduplex mobility assay initially and confirmed by sequencing of targeting sites. The heterozygous F1 were backcrossed to wild-type zebrafish (AB line; none of their own parents) to obtain F2. The F2 adult zebrafish carrying the same mutation were inter-crossed to generate the F3 offspring, which should contain wild-type (+/+), heterozygote (+/−), and homozygote (−/−) zebrafish. The primers used for mutant identification are listed in Table S1.

The three novel mutants were named according to zebrafish nomenclature guidelines: (https://zfin.org/ZDB-ALT-180803-3): $egln1a^{ihb1228/ihb12284}$ (M1), (https://zfin.org/ZDB-ALT-180803-4): $egln1b^{ihb1229/ihb1229}$ (M1), and (https://zfin.org/ZDB-ALT-180803-5): $egln3^{ihb1230/ihb1230}$. $egln1a^{ihb1228/ihb1228}$

egln1b$^{ihb1229/ihb1229}$ (*egln1a*$^{-/-}$/*1b*$^{-/-}$) double mutants were obtained by crossing *egln1a*$^{ihb1228/ihb1228}$ (M1) with *egln1b*$^{ihb1229/ihb1229}$ (M1). *Vhl*$^{-/-}$ has been described previously (10).

Dot blot assays for validation of anti TET2/3-OH antibody

The peptide solutions were spotted onto nitrocellulose membrane (1 μl). The membranes were dried for 1 h at 37 °C and blocked with 5% nonfat milk–Tris-buffered saline with Tween at room temperature for 2 h, then incubated with anti-TET2-OH, anti-TET3-OH, or antibody overnight at 4 °C. After washing three times with 5% nonfat milk, the membranes were incubated with HRP-conjugated secondary antibody for 1 h. Subsequently, the membranes were washed for three times with 5% nonfat milk and once with TBS and then visualized using an enhanced chemiluminescence detection kit (Millipore). Fuji Film LAS4000 mini luminescent image analyzer was used for photographing the blots.

Peptide pull-down assays

Peptide pull-down assays were performed as described previously with some modifications (11, 55). The biotinylated peptides were synthesized in Bioyeargene Biosciences (Wuhan, China). Briefly, the peptides (1 μg) were incubated with 1 mg of cell extracts (1 ml in volume) overnight at 4 °C and then added to 10 μl of streptavidin agarose (catalog no. 20347, Thermo Fisher Scientific) for 1 h at 4 °C. The agarose beads were washed four times with radioimmune precipitation assay buffer. Bound proteins were eluted by boiling in 1× SDS loading buffer for 5 min and then resolved by SDS-PAGE.

Statistical analysis

Semi-quantitative RT-PCR data are reported as mean ± S.D. of three independent experiments performed in triplicate. The statistical analysis was performed using GraphPad Prism 5 (unpaired *t* test) (GraphPad Software Inc.)

Data availability

All data generated during this study are included in this article and in the supporting information.

Acknowledgments—We are grateful to Drs Guoliang Xu and Peter J. Ratcliffe for the generous gift of reagents and cell lines.

Author contributions—S. F. and J. W. performed most of the experiments; G. Y. generated phd2-null and phd3-null zebrafish. D. Z. provided vhl-null zebrafish. F. R., X. Z., J. D., and Z. L. performed partial experiments or constructed some vectors. W. X. and J. W. directed the project, designed the experiments, analyzed data, and wrote the manuscript.

Funding and additional information—This work was supported by the strategic priority research program of the Chinese Academy of Sciences Grant XDA24010308 (to W. X.), National Natural Science Foundation of China Grants 31830101, 31721005, and 31671315 (to W. X.), and MOST National Key Research and Development Program of China Grant 2018YFD0900602 (to W. X.).

Conflict of interest—The authors declare that they have no conflicts of interest with the contents of this article.

Abbreviations—The abbreviations used are: VHL, von Hippel-Lindau; pVHL, VHL tumor suppressor; PHD, prolyl hydroxylase domain; TET, ten-eleven translocation; ccRCC, clear cell renal cell carcinoma; VCB, VHL with Elongin B and Elongin C; HIF, hypoxia-induced factor; 5-hmC, 5-hydroxymethylcytosine; 2ME2, 2-methoxyestradiol; CMV, cytomegalovirus; LAP, leukemia-associated protein; DMOG, dimethyloxalylglycine; CD, core-catalytic domain; MEF, mouse embryonic fibroblast; PBST, PBS with Tween.

References

1. Gossage, L., Eisen, T., and Maher, E. R. (2015) VHL, the story of a tumour suppressor gene. *Nat. Rev. Cancer* **15,** 55–64 CrossRef Medline
2. Shen, C., and Kaelin, W. G. Jr (2013) The VHL/HIF axis in clear cell renal carcinoma. *Semin. Cancer Biol.* **23,** 18–25 CrossRef Medline
3. Semenza, G. L. (2012) Hypoxia-inducible factors in physiology and medicine. *Cell* **148,** 399–408 CrossRef Medline
4. Majmundar, A. J., Wong, W. J., and Simon, M. C. (2010) Hypoxia-inducible factors and the response to hypoxic stress. *Mol. Cell* **40,** 294–309 CrossRef Medline
5. Jung, Y. S., Lee, S. J., Yoon, M. H., Ha, N. C., and Park, B. J. (2012) Estrogen receptor α is a novel target of the Von Hippel-Lindau protein and is responsible for the proliferation of VHL-deficient cells under hypoxic conditions. *Cell Cycle* **11,** 4462–4473 CrossRef Medline
6. Gamper, A. M., Qiao, X., Kim, J., Zhang, L., DeSimone, M. C., Rathmell, W. K., and Wan, Y. (2012) Regulation of KLF4 turnover reveals an unexpected tissue-specific role of pVHL in tumorigenesis. *Mol. Cell* **45,** 233–243 CrossRef Medline
7. Arias-González, L., Moreno-Gimeno, I., del Campo, A. R., Serrano-Oviedo, L., Valero, M. L., Esparís-Ogando, A., de la Cruz-Morcillo, M. A., Melgar-Rojas, P., García-Cano, J., Cimas, F. J., Hidalgo, M. J. R., Prado, A., Callejas-Valera, J. L., Nam-Cha, S. H., Giménez-Bachs, J. M., *et al.* (2013) ERK5/BMK1 is a novel target of the tumor suppressor VHL: implication in clear cell renal carcinoma. *Neoplasia* **15,** 649–659 CrossRef Medline
8. Huerta-Sánchez, E., Jin, X., Asan, Bianba, Z., Peter, B. M., Vinckenbosch, N., Liang, Y., Yi, X., He, M., Somel, M., Ni, P., Wang, B., Ou, X., Huasang, Luosang, J., Cuo, Z. X., Li, K., *et al.* (2014) Altitude adaptation in Tibetans caused by introgression of Denisovan-like DNA. *Nature* **512,** 194–197 CrossRef Medline
9. Wang, J., Zhang, W., Ji, W., Liu, X., Ouyang, G., and Xiao, W. (2014) The von Hippel-Lindau protein suppresses androgen receptor activity. *Mol. Endocrinol.* **28,** 239–248 CrossRef Medline
10. Du, J., Zhang, D., Zhang, W., Ouyang, G., Wang, J., Liu, X., Li, S., Ji, W., Liu, W., and Xiao, W. (2015) pVHL negatively regulates antiviral signaling by targeting MAVS for proteasomal degradation. *J. Immunol.* **195,** 1782–1790 CrossRef Medline
11. Guo, J. P., Chakraborty, A. A., Liu, P. D., Gan, W. J., Zheng, X. N., Inuzuka, H., Wang, B., Zhang, J. F., Zhang, L. L., Yuan, M., Novak, J., Cheng, J. Q., Toker, A., Signoretti, S., Zhang, Q., *et al.* (2016) pVHL suppresses kinase activity of Akt in a proline-hydroxylation-dependent manner. *Science* **353,** 929–932 CrossRef Medline
12. Zhang, J., Wu, T., Simon, J., Takada, M., Saito, R., Fan, C., Liu, X. D., Jonasch, E., Xie, L., Chen, X., Yao, X., Teh, B. T., Tan, P., Zheng, X., Li, M., *et al.* (2018) VHL substrate transcription factor ZHX2 as an oncogenic driver in clear cell renal cell carcinoma. *Science* **361,** 290–295 CrossRef Medline
13. Lian, C. G., Xu, Y., Ceol, C., Wu, F., Larson, A., Dresser, K., Xu, W., Tan, L., Hu, Y., Zhan, Q., Lee, C. W., Hu, D., Lian, B. Q., Kleffel, S., Yang, Y., *et al.* (2012) Loss of 5-hydroxymethylcytosine is an epigenetic hallmark of melanoma. *Cell* **150,** 1135–1146 CrossRef Medline
14. Schito, L., and Semenza, G. L. (2016) Hypoxia-inducible factors: master regulators of cancer progression. *Trends Cancer* **2,** 758–770 CrossRef Medline

15. Mariani, C. J., Vasanthakumar, A., Madzo, J., Yesilkanal, A., Bhagat, T., Yu, Y., Bhattacharyya, S., Wenger, R. H., Cohn, S. L., Nanduri, J., Verma, A., Prabhakar, N. R., and Godley, L. A. (2014) TET1-mediated hydroxymethylation facilitates hypoxic gene induction in neuroblastoma. *Cell Rep.* **7,** 1343–1352 CrossRef Medline
16. Liu, Q. Y., Liu, L., Zhao, Y. H., Zhang, J., Wang, D. F., Chen, J. W., He, Y. M., Wu, J. G., Zhang, Z. L., and Liu, Z. S. (2011) Hypoxia induces genomic DNA demethylation through the activation of HIF-1 α and transcriptional upregulation of MAT2A in hepatoma cells. *Mol. Cancer Ther.* **10,** 1113–1123 CrossRef Medline
17. Shahrzad, S., Bertrand, K., Minhas, K., and Coomber, B. L. (2007) Induction of DNA hypomethylation by tumor hypoxia. *Epigenetics* **2,** 119–125 CrossRef Medline
18. Skowronski, K., Dubey, S., Rodenhiser, D., and Coomber, B. L. (2010) Ischemia dysregulates DNA methyltransferases and *p16INK4a* methylation in human colorectal cancer cells. *Epigenetics* **5,** 547–556 CrossRef
19. Thienpont, B., Steinbacher, J., Zhao, H., D'Anna, F., Kuchnio, A., Ploumakis, A., Ghesquière, B., Van Dyck, L., Boeckx, B., Schoonjans, L., Hermans, E., Amant, F., Kristensen, V. N., Peng Koh, K., Mazzone, M., *et al.* (2016) Tumour hypoxia causes DNA hypermethylation by reducing TET activity. *Nature* **537,** 63–68 CrossRef Medline
20. Hattori, M., Yokoyama, Y., Hattori, T., Motegi, S., Amano, H., Hatada, I., and Ishikawa, O. (2015) Global DNA hypomethylation and hypoxia-induced expression of the ten eleven translocation (TET) family, TET1, in scleroderma fibroblasts. *Exp. Dermatol.* **24,** 841–846 CrossRef Medline
21. Wu, M. Z., Chen, S. F., Nieh, S., Benner, C., Ger, L. P., Jan, C. I., Ma, L., Chen, C. H., Hishida, T., Chang, H. T., Lin, Y. S., Montserrat, N., Gascon, P., Sancho-Martinez, I., and Izpisua Belmonte, J. C. (2015) Hypoxia drives breast tumor malignancy through a TET-TNFα-p38-MAPK signaling axis. *Cancer Res.* **75,** 3912–3924 CrossRef Medline
22. Querbes, W., Bogorad, R., Moslehi, J., Akinc, A., Wong, J., Zurenko, C., Qin, J., Hettinger, J., Kuchimanchi, S., Charisse, K., Sah, D. W. Y., Fitzgerald, K., Kotelianski, V., and Kaelin, W. G. (2011) Liver specific delivery of siRNA targeting EGLN prolyl hydroxylases activates hepatic erythropoietin production and stimulates erythropoiesis. *Blood* **118,** 3161 CrossRef
23. Tahiliani, M., Koh, K. P., Shen, Y. H., Pastor, W. A., Bandukwala, H., Brudno, Y., Agarwal, S., Iyer, L. M., Liu, D. R., Aravind, L., and Rao, A. (2009) Conversion of 5-methylcytosine to 5-hydroxymethylcytosine in mammalian DNA by MLL partner TET1. *Science* **324,** 930–935 CrossRef Medline
24. Gu, T. P., Guo, F., Yang, H., Wu, H. P., Xu, G. F., Liu, W., Xie, Z. G., Shi, L. Y., He, X. Y., Jin, S. G., Iqbal, K., Shi, Y. J. G., Deng, Z. X., Szabo, P. E., Pfeifer, G. P., *et al.* (2011) The role of Tet3 DNA dioxygenase in epigenetic reprogramming by oocytes. *Nature* **477,** 606–610 CrossRef Medline
25. Ito, S., D'Alessio, A. C., Taranova, O. V., Hong, K., Sowers, L. C., and Zhang, Y. (2010) Role of Tet proteins in 5mC to 5hmC conversion, ES-cell self-renewal and inner cell mass specification. *Nature* **466,** 1129–1133 CrossRef Medline
26. Wu, H., and Zhang, Y. (2011) Mechanisms and functions of Tet protein-mediated 5-methylcytosine oxidation. *Genes Dev.* **25,** 2436–2452 CrossRef Medline
27. Rasmussen, K. D., and Helin, K. (2016) Role of TET enzymes in DNA methylation, development, and cancer. *Genes Dev.* **30,** 733–750 CrossRef Medline
28. Tsai, Y. P., Chen, H. F., Chen, S. Y., Cheng, W. C., Wang, H. W., Shen, Z. J., Song, C., Teng, S. C., He, C., and Wu, K. J. (2014) TET1 regulates hypoxia-induced epithelial-mesenchymal transition by acting as a co-activator. *Genome Biol.* **15,** 513 CrossRef Medline
29. Wang, J., Zhang, D. W., Du, J., Zhou, C., Li, Z., Liu, X., Ouyang, G., and Xiao, W. H. (2017) Tet1 facilitates hypoxia tolerance by stabilizing the HIF-α proteins independent of its methylcytosine dioxygenase activity. *Nucleic Acids Res.* **45,** 12700–12714 CrossRef
30. Laukka, T., Mariani, C. J., Ihantola, T., Cao, J. Z., Hokkanen, J., Kaelin, W. G., Godley, L. A., and Koivunen, P. (2016) Fumarate and succinate regulate expression of hypoxia-inducible genes via TET enzymes. *J. Biol. Chem.* **291,** 4256–4265 CrossRef Medline
31. Ko, M., An, J., Bandukwala, H. S., Chavez, L., Aijö, T., Pastor, W. A., Segal, M. F., Li, H. M., Koh, K. P., Lähdesmäki, H., Hogan, P. G., Aravind, L., and Rao, A. (2013) Modulation of TET2 expression and 5-methylcytosine oxidation by the CXXC domain protein IDAX. *Nature* **497,** 122–126 CrossRef Medline
32. Shi, F. T., Kim, H., Lu, W., He, Q., Liu, D., Goodell, M. A., Wan, M., and Songyang, Z. (2013) Ten-eleven translocation 1 (Tet1) is regulated by O-linked N-acetylglucosamine transferase (Ogt) for target gene repression in mouse embryonic stem cells. *J. Biol. Chem.* **288,** 20776–20784 CrossRef Medline
33. Yu, C., Zhang, Y. L., Pan, W. W., Li, X. M., Wang, Z. W., Ge, Z. J., Zhou, J. J., Cang, Y., Tong, C., Sun, Q. Y., and Fan, H. Y. (2013) CRL4 complex regulates mammalian oocyte survival and reprogramming by activation of TET proteins. *Science* **342,** 1518–1521 CrossRef Medline
34. Wang, Y., and Zhang, Y. (2014) Regulation of TET protein stability by calpains. *Cell Rep.* **6,** 278–284 CrossRef Medline
35. Nakagawa, T., Lv, L., Nakagawa, M., Yu, Y., Yu, C., D'Alessio, A. C., Nakayama, K., Fan, H. Y., Chen, X., and Xiong, Y. (2015) CRL4(VprBP) E3 ligase promotes monoubiquitylation and chromatin binding of TET dioxygenases. *Mol. Cell* **57,** 247–260 CrossRef Medline
36. Bauer, C., Göbel, K., Nagaraj, N., Colantuoni, C., Wang, M., Müller, U., Kremmer, E., Rottach, A., and Leonhardt, H. (2015) Phosphorylation of TET proteins is regulated via O-GlcNAcylation by the O-linked N-acetylglucosamine transferase (OGT). *J. Biol. Chem.* **290,** 4801–4812 CrossRef Medline
37. Zhang, Y. W., Wang, Z., Xie, W., Cai, Y., Xia, L., Easwaran, H., Luo, J., Yen, R. C., Li, Y., and Baylin, S. B. (2017) Acetylation enhances TET2 function in protecting against abnormal DNA methylation during oxidative stress. *Mol. Cell* **65,** 323–335 CrossRef Medline
38. Bhattacharyya, S., Yu, H., Mim, C., and Matouschek, A. (2014) Regulated protein turnover: snapshots of the proteasome in action. *Nat. Rev. Mol. Cell Biol.* **15,** 122–133 CrossRef Medline
39. Geng, F., Wenzel, S., and Tansey, W. P. (2012) Ubiquitin and proteasomes in transcription. *Annu. Rev. Biochem.* **81,** 177–201 CrossRef Medline
40. Ivan, M., and Kaelin, W. G. Jr (2017) The EGLN-HIF O2-sensing system: multiple inputs and feedbacks. *Mol. Cell* **66,** 772–779 CrossRef Medline
41. Lin, G., Sun, W., Yang, Z., Guo, J., Liu, H., and Liang, J. (2017) Hypoxia induces the expression of TET enzymes in HepG2 cells. *Oncol. Lett.* **14,** 6457–6462 CrossRef Medline
42. Tanimoto, K., Makino, Y., Pereira, T., and Poellinger, L. (2000) Mechanism of regulation of the hypoxia-inducible factor-1 α by the von Hippel-Lindau tumor suppressor protein. *EMBO J.* **19,** 4298–4309 CrossRef Medline
43. Mabjeesh, N. J., Escuin, D., LaVallee, T. M., Pribluda, V. S., Swartz, G. M., Johnson, M. S., Willard, M. T., Zhong, H., Simons, J. W., and Giannakakou, P. (2003) 2ME2 inhibits tumor growth and angiogenesis by disrupting microtubules and dysregulating HIF. *Cancer Cell* **3,** 363–375 CrossRef Medline
44. Ito, S., Shen, L., Dai, Q., Wu, S. C., Collins, L. B., Swenberg, J. A., He, C., and Zhang, Y. (2011) Tet proteins can convert 5-methylcytosine to 5-formylcytosine and 5-carboxylcytosine. *Science* **333,** 1300–1303 CrossRef Medline
45. Hashimoto, H., Liu, Y., Upadhyay, A. K., Chang, Y., Howerton, S. B., Vertino, P. M., Zhang, X., and Cheng, X. (2012) Recognition and potential mechanisms for replication and erasure of cytosine hydroxymethylation. *Nucleic Acids Res.* **40,** 4841–4849 CrossRef Medline
46. Wu, H., and Zhang, Y. (2014) Reversing DNA methylation: mechanisms, genomics, and biological functions. *Cell* **156,** 45–68 CrossRef Medline
47. Schofield, C. J., and Ratcliffe, P. J. (2004) Oxygen sensing by HIF hydroxylases. *Nat. Rev. Mol. Cell Biol.* **5,** 343–354 CrossRef Medline
48. Mills, D. B., Francis, W. R., Vargas, S., Larsen, M., Elemans, C. P., Canfield, D. E., and Wörheide, G. (2018) The last common ancestor of animals lacked the HIF pathway and respired in low-oxygen environments. *eLife* **7,** e31176 CrossRef
49. Takeda, Y., Costa, S., Delamarre, E., Roncal, C., Leite de Oliveira, R., Squadrito, M. L., Finisguerra, V., Deschoemaeker, S., Bruyère, F., Wenes, M., Hamm, A., Serneels, J., Magat, J., Bhattacharyya, T., Anisimov, A., *et al.* (2011) Macrophage skewing by Phd2 haplodeficiency prevents ischaemia by inducing arteriogenesis. *Nature* **479,** 122–126 CrossRef Medline
50. Jokilehto, T., Högel, H., Heikkinen, P., Rantanen, K., Elenius, K., Sundström, J., and Jaakkola, P. M. (2010) Retention of prolyl hydroxylase PHD2

in the cytoplasm prevents PHD2-induced anchorage-independent carcinoma cell growth. *Exp. Cell Res.* **316,** 1169–1178 CrossRef Medline
51. Wang, J. C., Chan, R. C., Tsai, Y. A., Huang, W. C., Cheng, H., Wu, H. L., and Huang, S. F. (2015) The influence of shoulder pain on functional limitation, perceived health, and depressive mood in patients with traumatic paraplegia. *J. Spinal Cord Med.* **38,** 587–592 CrossRef
52. Henze, A. T., Garvalov, B. K., Seidel, S., Cuesta, A. M., Ritter, M., Filatova, A., Foss, F., Dopeso, H., Essmann, C. L., Maxwell, P. H., Reifenberger, G., Carmeliet, P., Acker-Palmer, A., and Acker, T. (2014) Loss of PHD3 allows tumours to overcome hypoxic growth inhibition and sustain proliferation through EGFR. *Nat. Commun.* **5,** 5582 CrossRef Medline
53. Botusan, I. R., Sunkari, V. G., Savu, O., Catrina, A. I., Grünler, J., Lindberg, S., Pereira, T., Ylä-Herttuala, S., Poellinger, L., Brismar, K., and Catrina, S. B. (2008) Stabilization of HIF-1α is critical to improve wound healing in diabetic mice. *Proc. Natl. Acad. Sci. U. S. A.* **105,** 19426–19431 CrossRef Medline
54. Pastor, W. A., Aravind, L., and Rao, A. (2013) TETonic shift: biological roles of TET proteins in DNA demethylation and transcription. *Nat. Rev. Mol. Cell Biol.* **14,** 341–356 CrossRef Medline
55. Zheng, X. N., Zhai, B., Koivunen, P., Shin, S. J., Lu, G., Liu, J. Y., Geisen, C., Chakraborty, A. A., Moslehi, J. J., Smalley, D. M., Wei, X., Chen, X., Chen, Z. M., Beres, J. M., Zhang, J., *et al.* (2014) Prolyl hydroxylation by EglN2 destabilizes FOXO3a by blocking its interaction with the USP9x deubiquitinase. *Genes Dev.* **28,** 1429–1444 CrossRef Medline
56. Esteban, M. A., Tran, M. G., Harten, S. K., Hill, P., Castellanos, M. C., Chandra, A., Raval, R., O'Brien, T. S., and Maxwell, P. H. (2006) Regulation of E-cadherin expression by VHL and hypoxia-inducible factor. *Cancer Res.* **66,** 3567–3575 CrossRef Medline
57. Noonan, H. R., Metelo, A. M., Kamei, C. N., Peterson, R. T., Drummond, I. A., and Iliopoulos, O. (2016) Loss of vhl in the zebrafish pronephros recapitulates early stages of human clear cell renal cell carcinoma. *Dis. Model Mech.* **9,** 873–884 CrossRef Medline
58. Li, C., Lan, Y., Schwartz-Orbach, L., Korol, E., Tahiliani, M., Evans, T., and Goll, M. G. (2015) Overlapping requirements for Tet2 and Tet3 in normal development and hematopoietic stem cell emergence. *Cell Rep.* **12,** 1133–1143 CrossRef Medline
59. Ehrlich, M. (2009) DNA hypomethylation in cancer cells. *Epigenomics* **1,** 239–259 CrossRef Medline
60. Friso, S., Udali, S., Guarini, P., Pellegrini, C., Pattini, P., Moruzzi, S., Girelli, D., Pizzolo, F., Martinelli, N., Corrocher, R., Olivieri, O., and Choi, S. W. (2013) Global DNA hypomethylation in peripheral blood mononuclear cells as a biomarker of cancer risk. *Cancer Epidemiol. Biomarkers Prev.* **22,** 348–355 CrossRef Medline
61. Yang, L., Rodriguez, B., Mayle, A., Park, H. J., Lin, X., Luo, M., Jeong, M., Curry, C. V., Kim, S. B., Ruau, D., Zhang, X., Zhou, T., Zhou, M., Rebel, V. I., Challen, G. A., *et al.* (2016) DNMT3A loss drives enhancer hypomethylation in FLT3-ITD-associated leukemias. *Cancer Cell* **29,** 922–934 CrossRef Medline
62. Mendoza-Perez, J., Gu, J., Herrera, L. A., Tannir, N. M., Matin, S. F., Karam, J. A., Huang, M., Chang, D. W., Wood, C. G., and Wu, X. (2016) Genomic DNA hypomethylation and risk of renal cell carcinoma: a case-control study. *Clin. Cancer Res.* **22,** 2074–2082 CrossRef Medline
63. Ludgate, J. L., Le Mée, G., Fukuzawa, R., Rodger, E. J., Weeks, R. J., Reeve, A. E., and Morison, I. M. (2013) Global demethylation in loss of imprinting subtype of Wilms tumor. *Genes Chromosomes Cancer* **52,** 174–184 CrossRef Medline
64. Artemov, A. V., Zhigalova, N., Zhenilo, S., Mazur, A. M., and Prokhortchouk, E. B. (2018) VHL inactivation without hypoxia is sufficient to achieve genome hypermethylation. *Sci. Rep.* **8,** 10667 CrossRef Medline
65. Robinson, C. M., Lefebvre, F., Poon, B. P., Bousard, A., Fan, X., Lathrop, M., Tost, J., Kim, W. Y., Riazalhosseini, Y., and Ohh, M. (2018) Consequences of VHL loss on global DNA methylome. *Sci. Rep.* **8,** 3313 CrossRef Medline
66. Maxwell, P. H., Wiesener, M. S., Chang, G. W., Clifford, S. C., Vaux, E. C., Cockman, M. E., Wykoff, C. C., Pugh, C. W., Maher, E. R., and Ratcliffe, P. J. (1999) The tumour suppressor protein VHL targets hypoxia-inducible factors for oxygen-dependent proteolysis. *Nature* **399,** 271–275 CrossRef Medline
67. Ivan, M., Kondo, K., Yang, H., Kim, W., Valiando, J., Ohh, M., Salic, A., Asara, J. M., Lane, W. S., and Kaelin, W. G. Jr (2001) HIFα targeted for VHL-mediated destruction by proline hydroxylation: implications for O_2 sensing. *Science* **292,** 464–468 CrossRef Medline
68. Jaakkola, P., Mole, D. R., Tian, Y. M., Wilson, M. I., Gielbert, J., Gaskell, S. J., von Kriegsheim, A., Hebestreit, H. F., Mukherji, M., Schofield, C. J., Maxwell, P. H., Pugh, C. W., and Ratcliffe, P. J. (2001) Targeting of HIF-α to the von Hippel-Lindau ubiquitylation complex by O_2-regulated prolyl hydroxylation. *Science* **292,** 468–472 CrossRef Medline
69. Kaelin, W. G. Jr (2008) The von Hippel-Lindau tumour suppressor protein: O2 sensing and cancer. *Nat. Rev. Cancer* **8,** 865–873 CrossRef Medline
70. Moser, S. C., Bensaddek, D., Ortmann, B., Maure, J. F., Mudie, S., Blow, J. J., Lamond, A. I., Swedlow, J. R., and Rocha, S. (2013) PHD1 links cell-cycle progression to oxygen sensing through hydroxylation of the centrosomal protein Cep192. *Dev. Cell* **26,** 381–392 CrossRef Medline
71. Cummins, E. P., Berra, E., Comerford, K. M., Ginouves, A., Fitzgerald, K. T., Seeballuck, F., Godson, C., Nielsen, J. E., Moynagh, P., Pouyssegur, J., and Taylor, C. T. (2006) Prolyl hydroxylase-1 negatively regulates IκB kinase-β, giving insight into hypoxia-induced NFκB activity. *Proc. Natl. Acad. Sci. U. S. A.* **103,** 18154–18159 CrossRef Medline
72. Luo, W., Hu, H., Chang, R., Zhong, J., Knabel, M., O'Meally, R., Cole, R. N., Pandey, A., and Semenza, G. L. (2011) Pyruvate kinase M2 is a PHD3-stimulated coactivator for hypoxia-inducible factor 1. *Cell* **145,** 732–744 CrossRef Medline
73. Liu, X., Chen, Z., Xu, C., Leng, X., Cao, H., Ouyang, G., and Xiao, W. (2015) Repression of hypoxia-inducible factor α signaling by Set7-mediated methylation. *Nucleic Acids Res.* **43,** 5081–5098 CrossRef Medline
74. Chen, Z., Liu, X., Mei, Z., Wang, Z., and Xiao, W. (2014) EAF2 suppresses hypoxia-induced factor 1α transcriptional activity by disrupting its interaction with coactivator CBP/p300. *Mol. Cell Biol.* **34,** 1085–1099 CrossRef Medline
75. Sajadian, S. O., Tripura, C., Samani, F. S., Ruoss, M., Dooley, S., Baharvand, H., and Nussler, A. K. (2016) Vitamin C enhances epigenetic modifications induced by 5-azacytidine and cell cycle arrest in the hepatocellular carcinoma cell lines HLE and Huh7. *Clin. Epigenetics* **8,** 46 CrossRef Medline
76. Ota, S., Hisano, Y., Muraki, M., Hoshijima, K., Dahlem, T. J., Grunwald, D. J., Okada, Y., and Kawahara, A. (2013) Efficient identification of TALEN-mediated genome modifications using heteroduplex mobility assays. *Genes Cells* **18,** 450–458 CrossRef Medline